# Sync-up

Qichen Huang
Paul François Lab

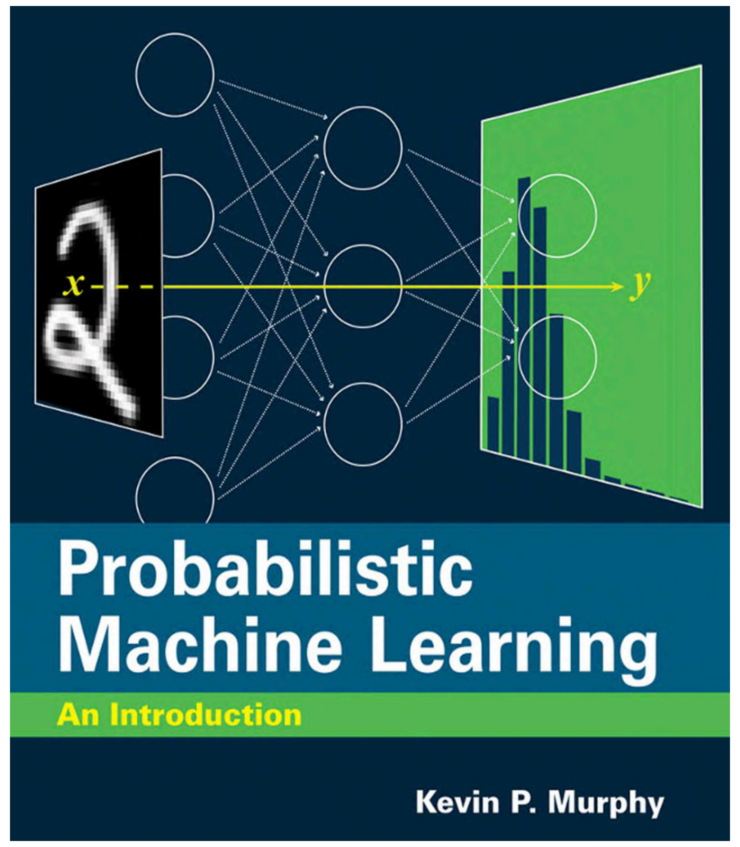

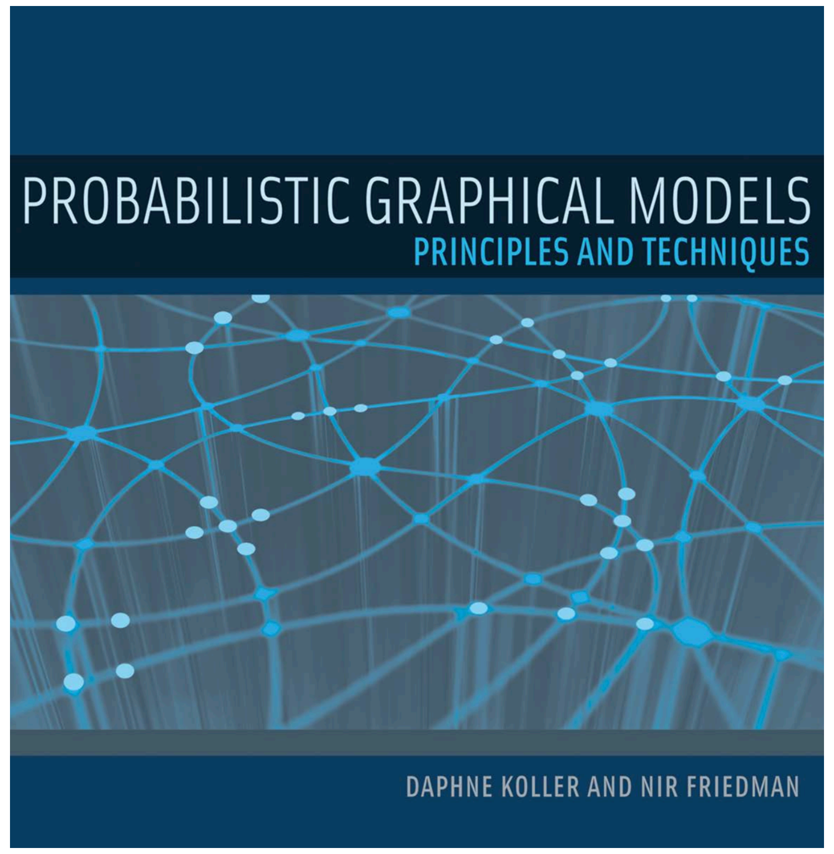

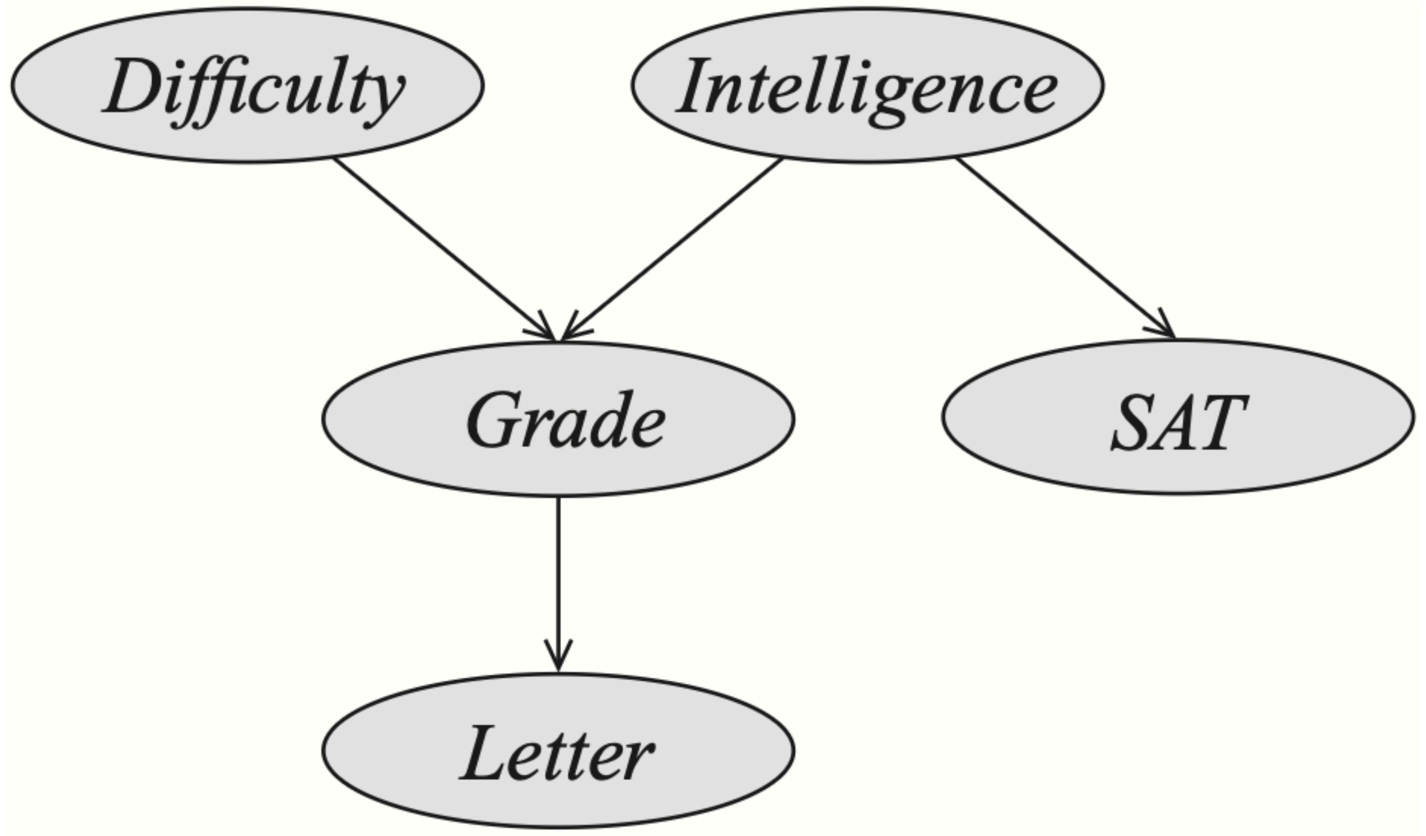

**Figure 3.3** **The Bayesian Network graph for the** Student **example**

Probabilistic ML
- Stochastic Processes
- Probabilistic Graphical Models
  - Bayesian Network, DAG
  - Dynamic Bayesian Network
    - Markov Decision Process, RL

....

- GFlowNets

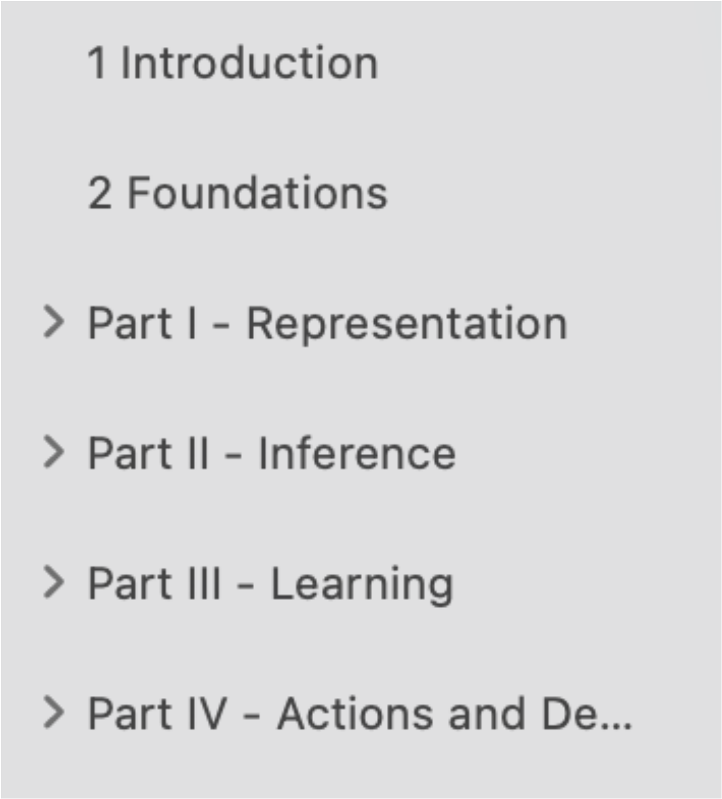
1 Introduction

2 Foundations

> Part I - Representation

> Part II - Inference

> Part III - Learning

> Part IV - Actions and De...

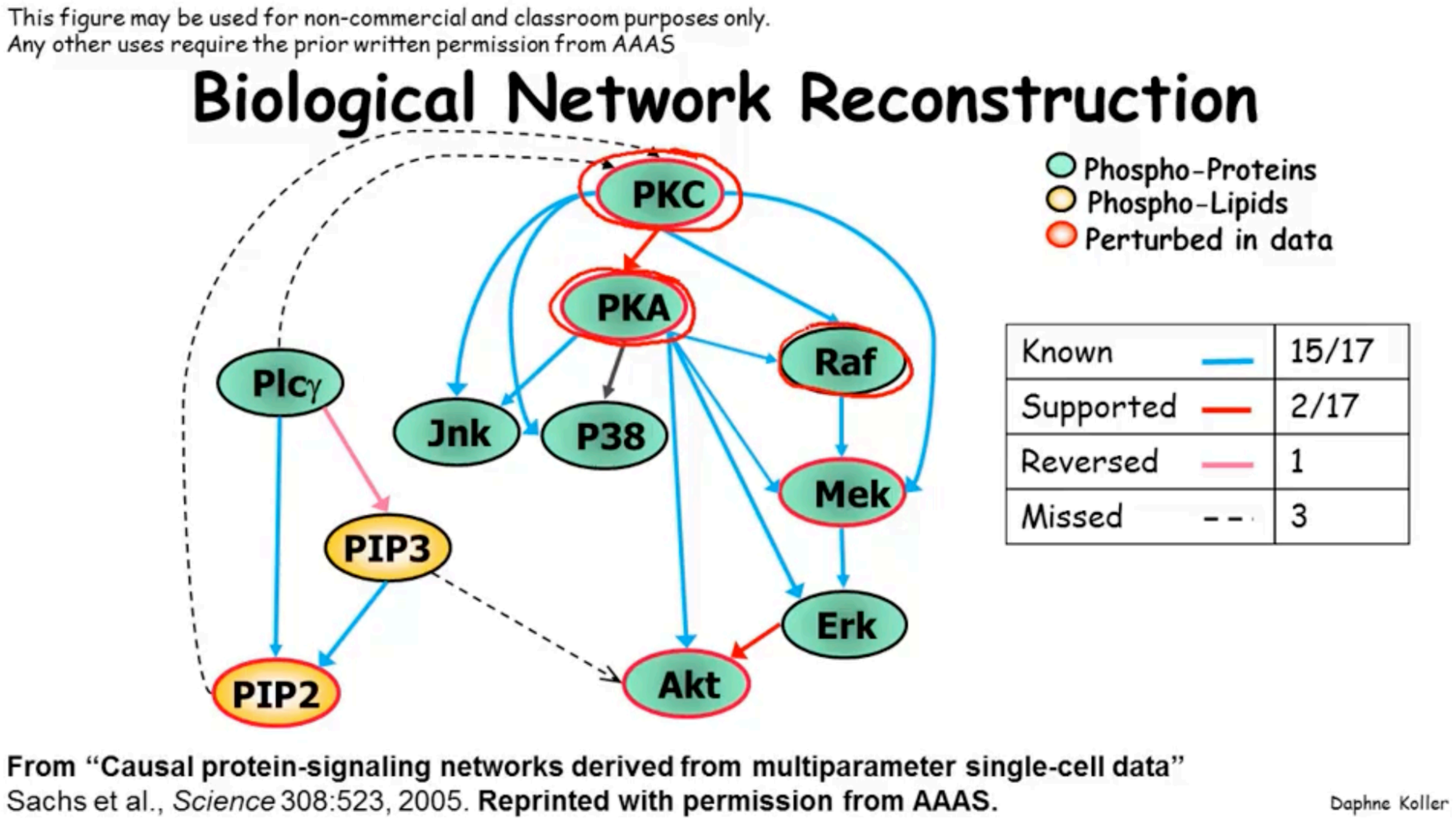
This figure may be used for non-commercial and classroom purposes only.
Any other uses require the prior written permission from AAAS

**Biological Network Reconstruction**

○ Phospho-Proteins
○ Phospho-Lipids
○ Perturbed in data

| | | |
|---|---|---|
| Known | — | 15/17 |
| Supported | — | 2/17 |
| Reversed | — | 1 |
| Missed | - - | 3 |

**From "Causal protein-signaling networks derived from multiparameter single-cell data"**
Sachs et al., *Science* 308:523, 2005. **Reprinted with permission from AAAS.**

Daphne Koller

Koller, D., & Friedman, N. (2009). Probabilistic graphical models: Principles and techniques. MIT Press.

# BIN60052

## Evolving Diverse Gene Networks

A case study on Somite Patterns during Embryonic Development

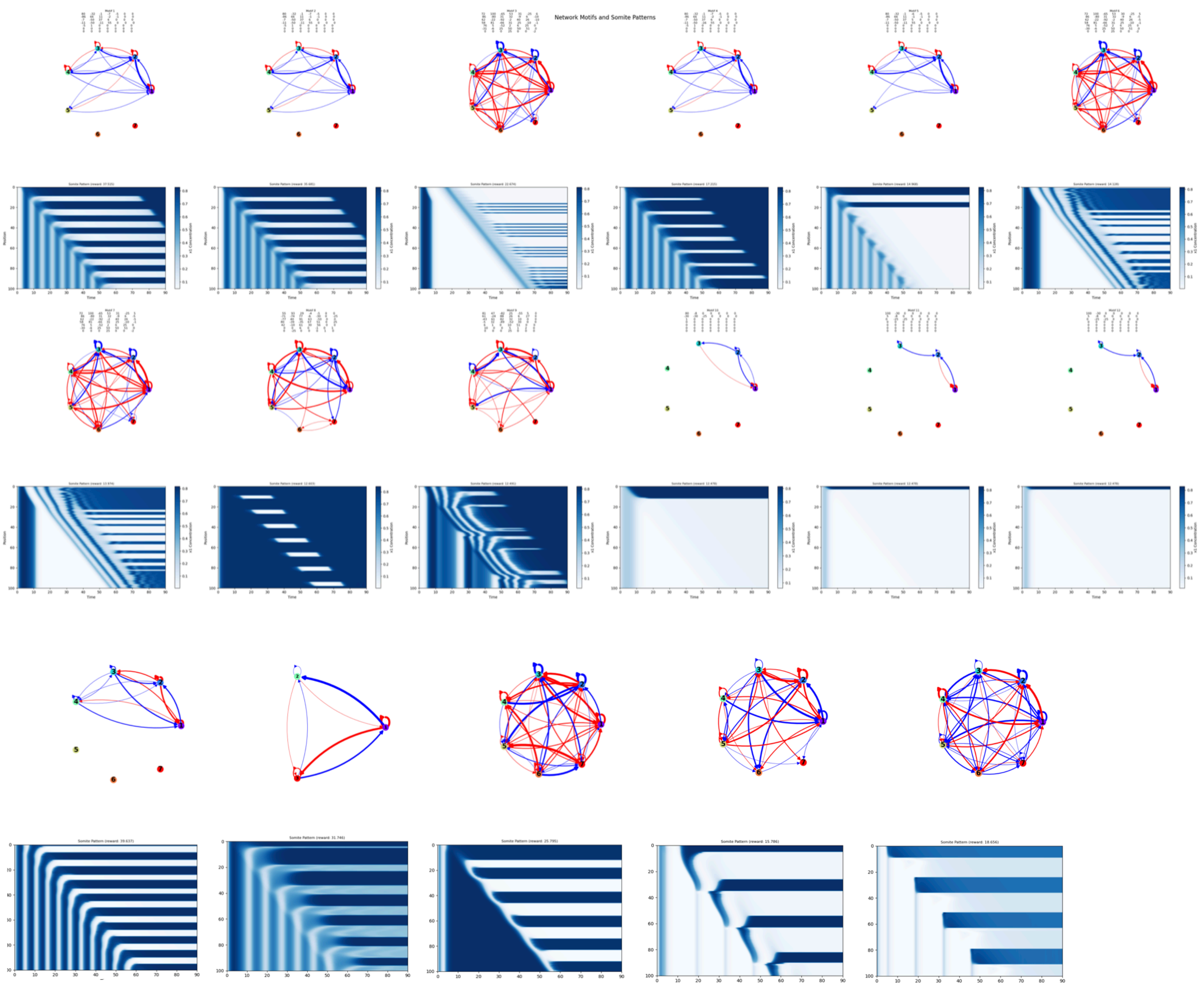

classical unequal unexpected smooth sharp

# BCM2003

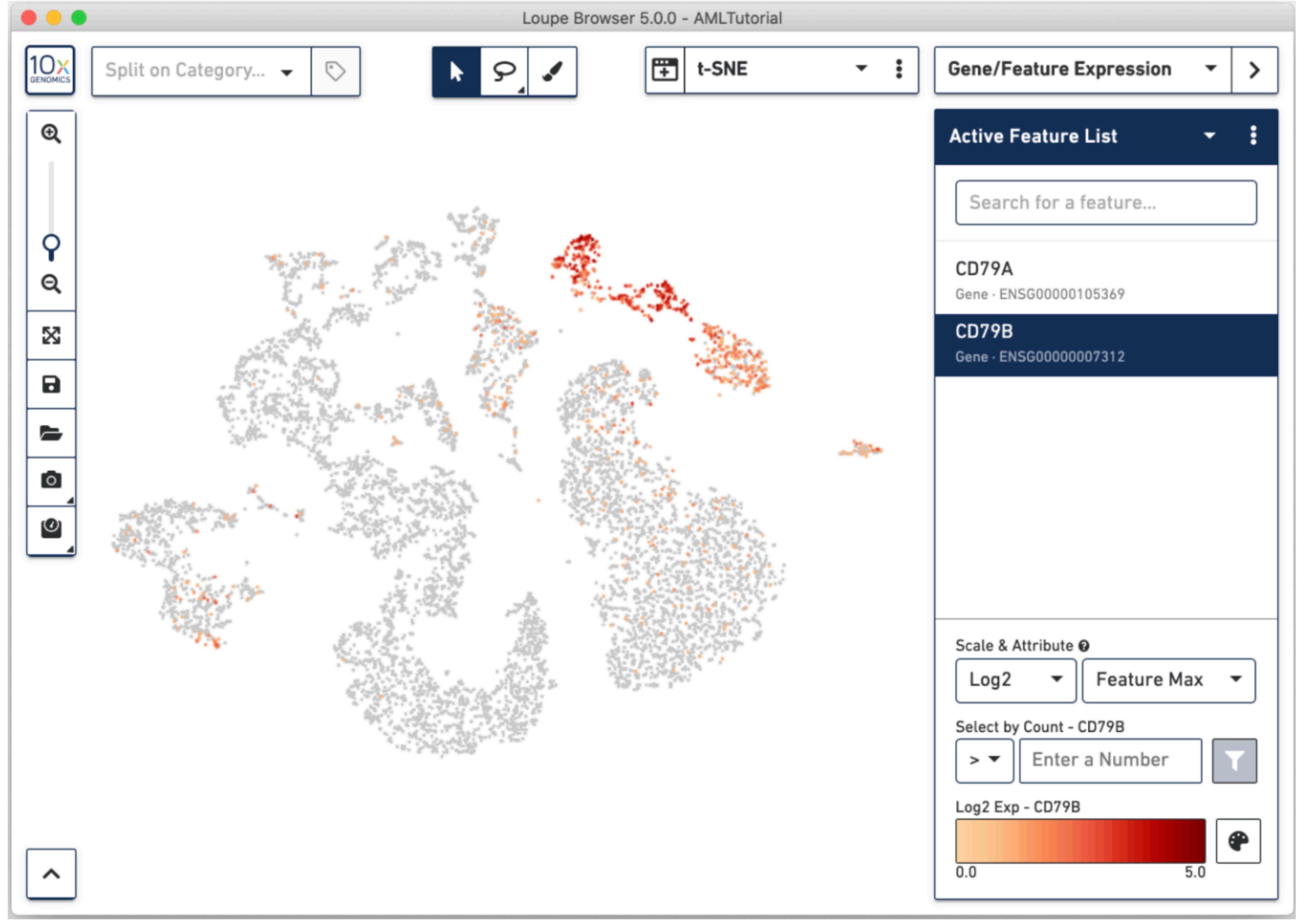

# IFT6164

## Adversarial Goodhart with LLMs

**Olivier Déry-Prévost**
`Olivier.dery-prevost@mila.quebec`

**Qichen Huang**
`qichen.huang@mila.quebec`

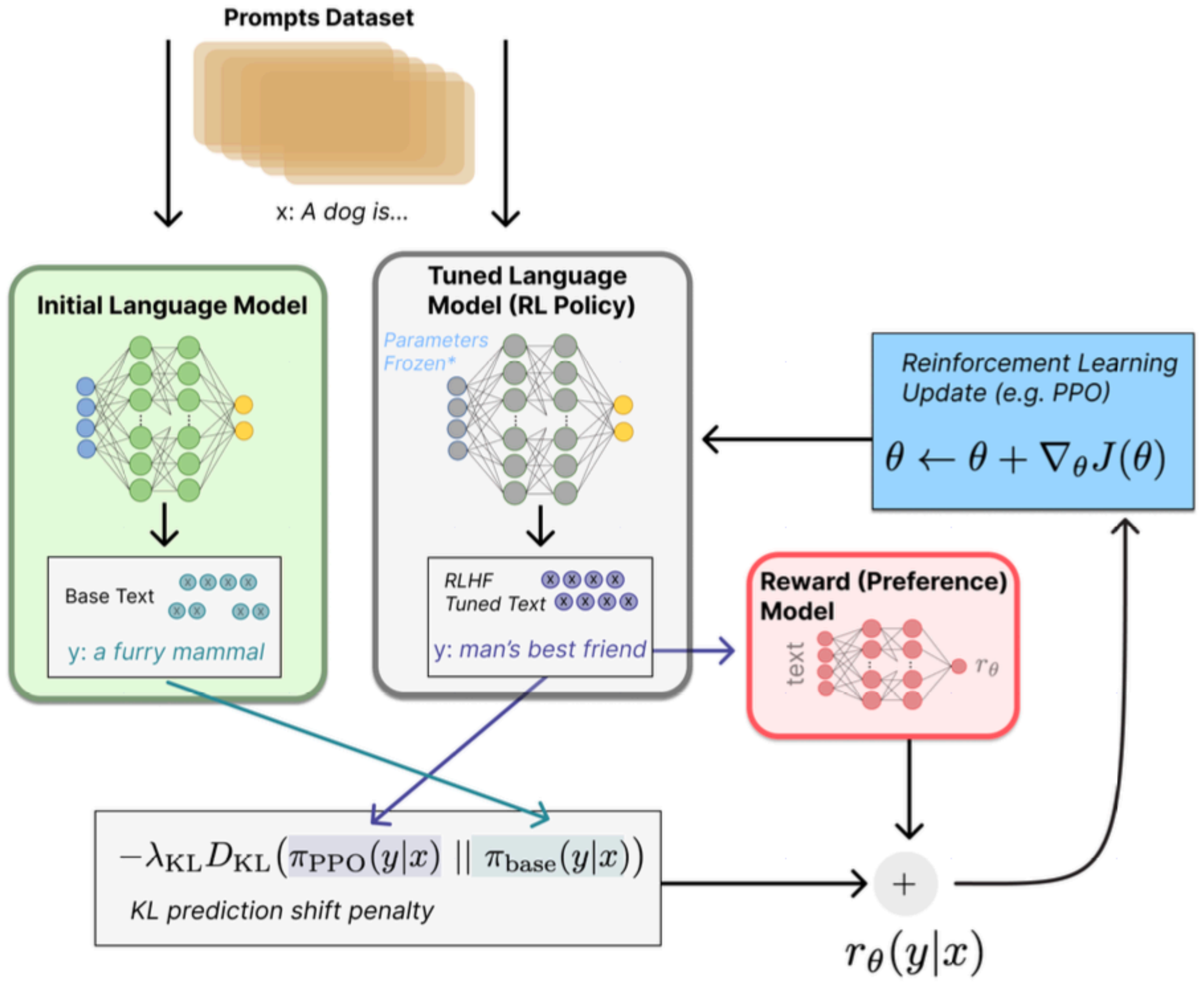

# BIN6001

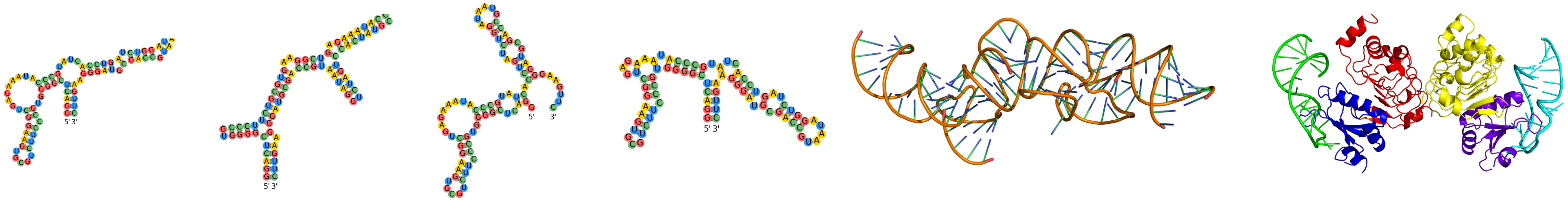


Become a Gary
Become a Jürgen
JUERGEN SCHMIDHUBER TURNED 60 IN 2023. STILL IN GOOD SHAPE
Become an Eliezer
Me, getting older
dingboard!

# Review GFN

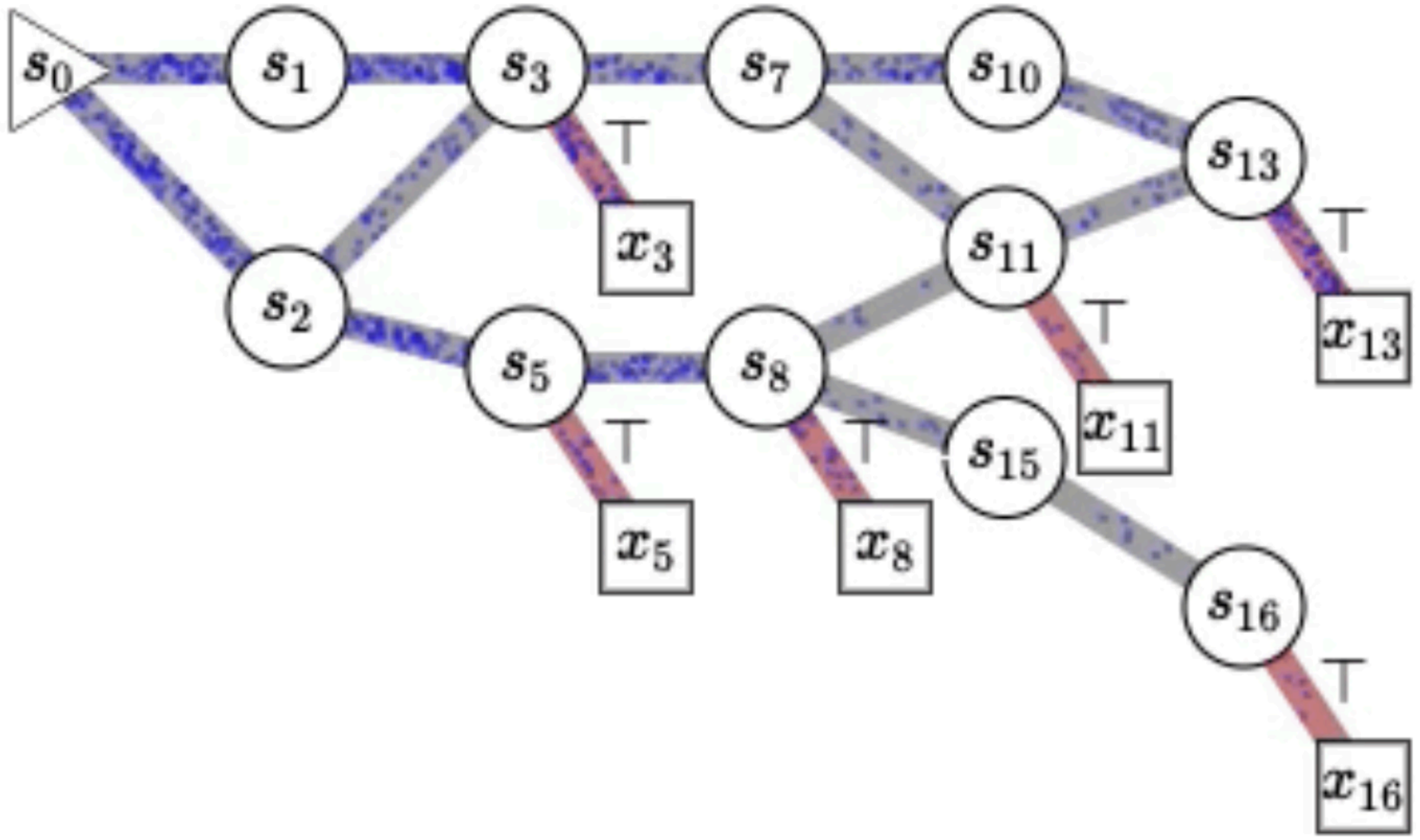

$$\pi(a|s) = \pi(s \rightarrow s' = T(s,a)|s) = P_F(s'|s) = \frac{F(s \rightarrow s')}{\sum_{s''} F(s \rightarrow s'')}.$$

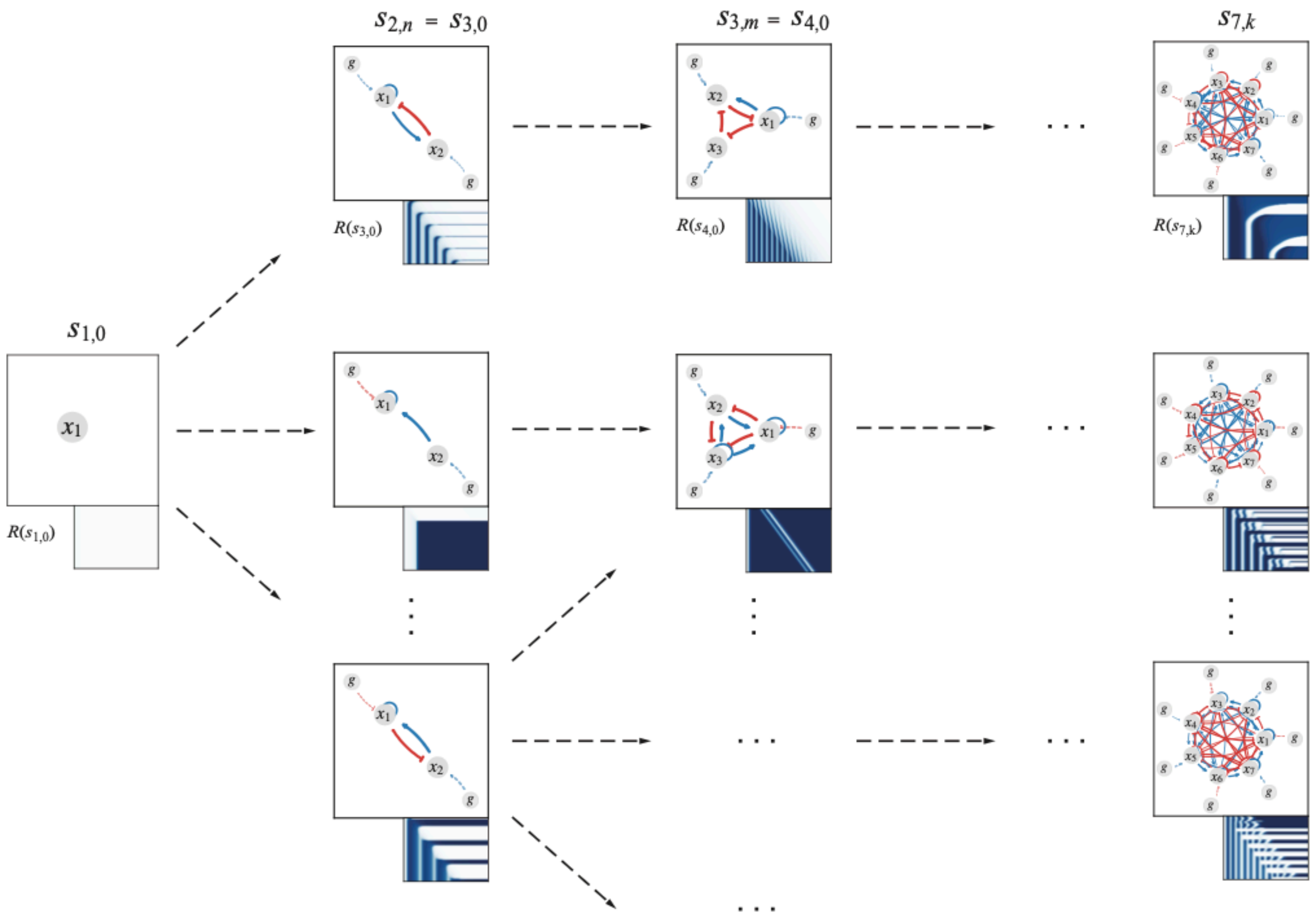

Figure 1: Illustration of the node-first search strategy. For a fixed number of nodes $i$, the GFlowNet updates edges within the subnetwork along a trajectory $s_{i,0} \rightarrow \cdots \rightarrow s_{i,T_i}$. When the subnetwork is explored, a new node is added and the search continues from $s_{i+1,0}$ with $s_{i,T_i} = s_{i+1,0}$. Each state is a motif and the reward $R(s_{i,k})$ computed from the simulated kymograph.

Trajectory Visualization: Network Motifs & Somite Patterns

Trajectory Reward Curve

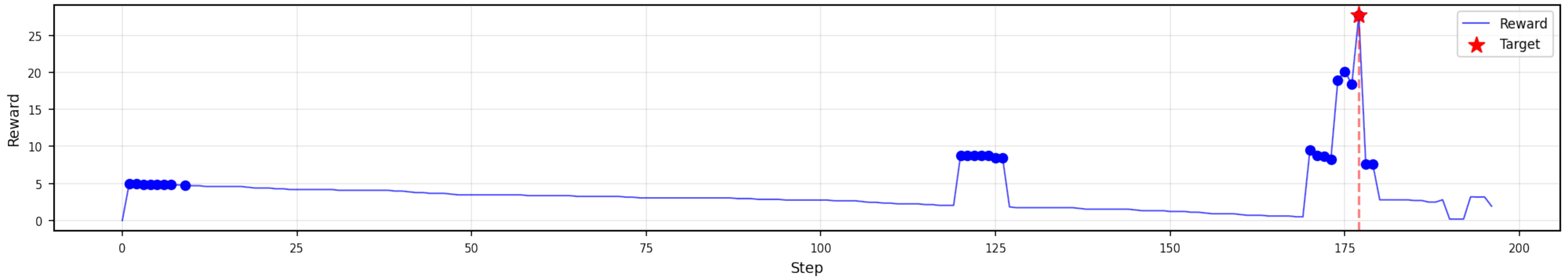

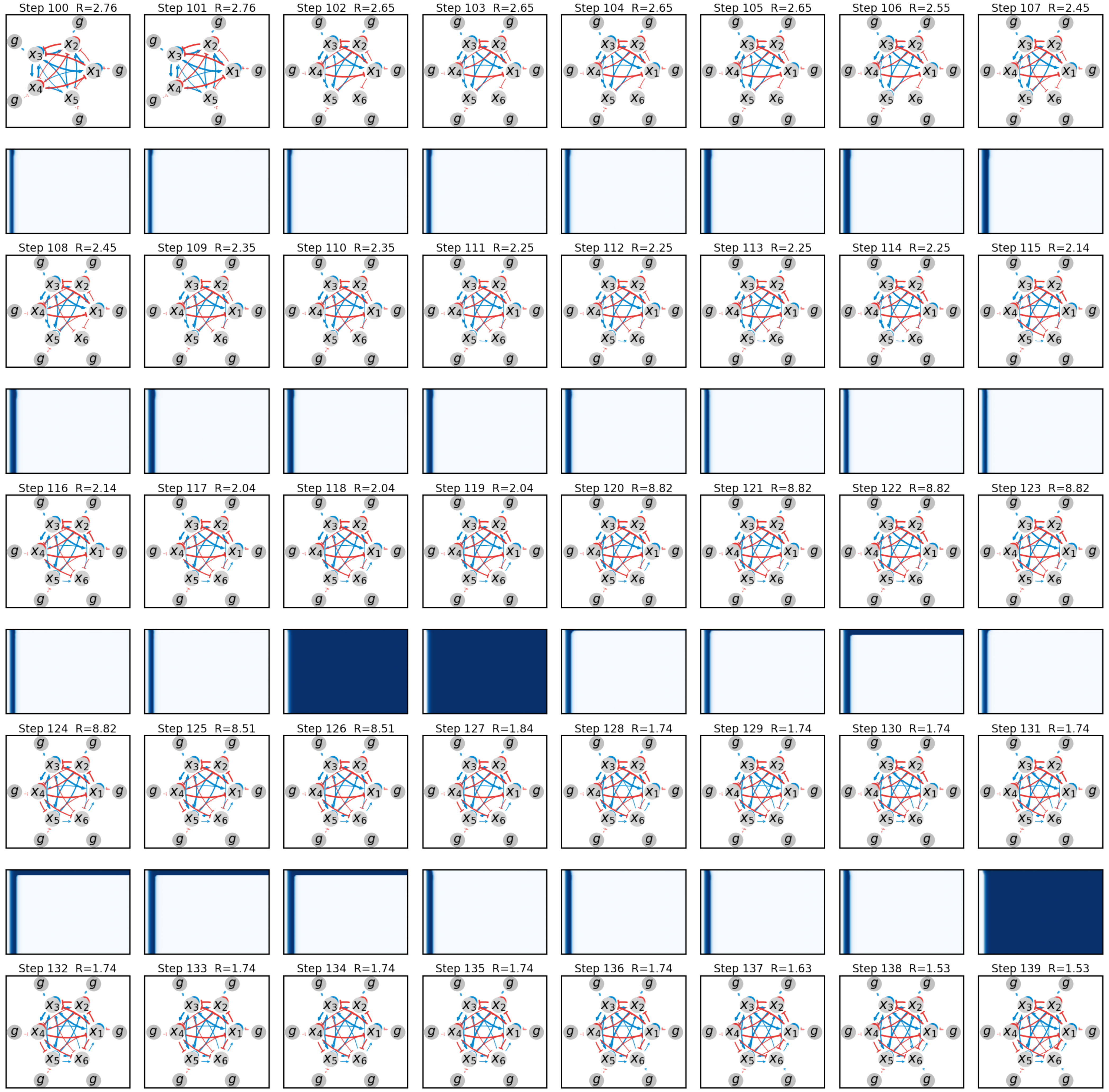
Step 100 R=2.76
Step 101 R=2.76
Step 102 R=2.65
Step 103 R=2.65
Step 104 R=2.65
Step 105 R=2.65
Step 106 R=2.55
Step 107 R=2.45
Step 108 R=2.45
Step 109 R=2.35
Step 110 R=2.35
Step 111 R=2.25
Step 112 R=2.25
Step 113 R=2.25
Step 114 R=2.25
Step 115 R=2.14
Step 116 R=2.14
Step 117 R=2.04
Step 118 R=2.04
Step 119 R=2.04
Step 120 R=8.82
Step 121 R=8.82
Step 122 R=8.82
Step 123 R=8.82
Step 124 R=8.82
Step 125 R=8.51
Step 126 R=8.51
Step 127 R=1.84
Step 128 R=1.74
Step 129 R=1.74
Step 130 R=1.74
Step 131 R=1.74
Step 132 R=1.74
Step 133 R=1.74
Step 134 R=1.74
Step 135 R=1.74
Step 136 R=1.74
Step 137 R=1.63
Step 138 R=1.53
Step 139 R=1.53
$x_1$
$x_2$
$x_3$
$x_4$
$x_5$
$x_6$
g

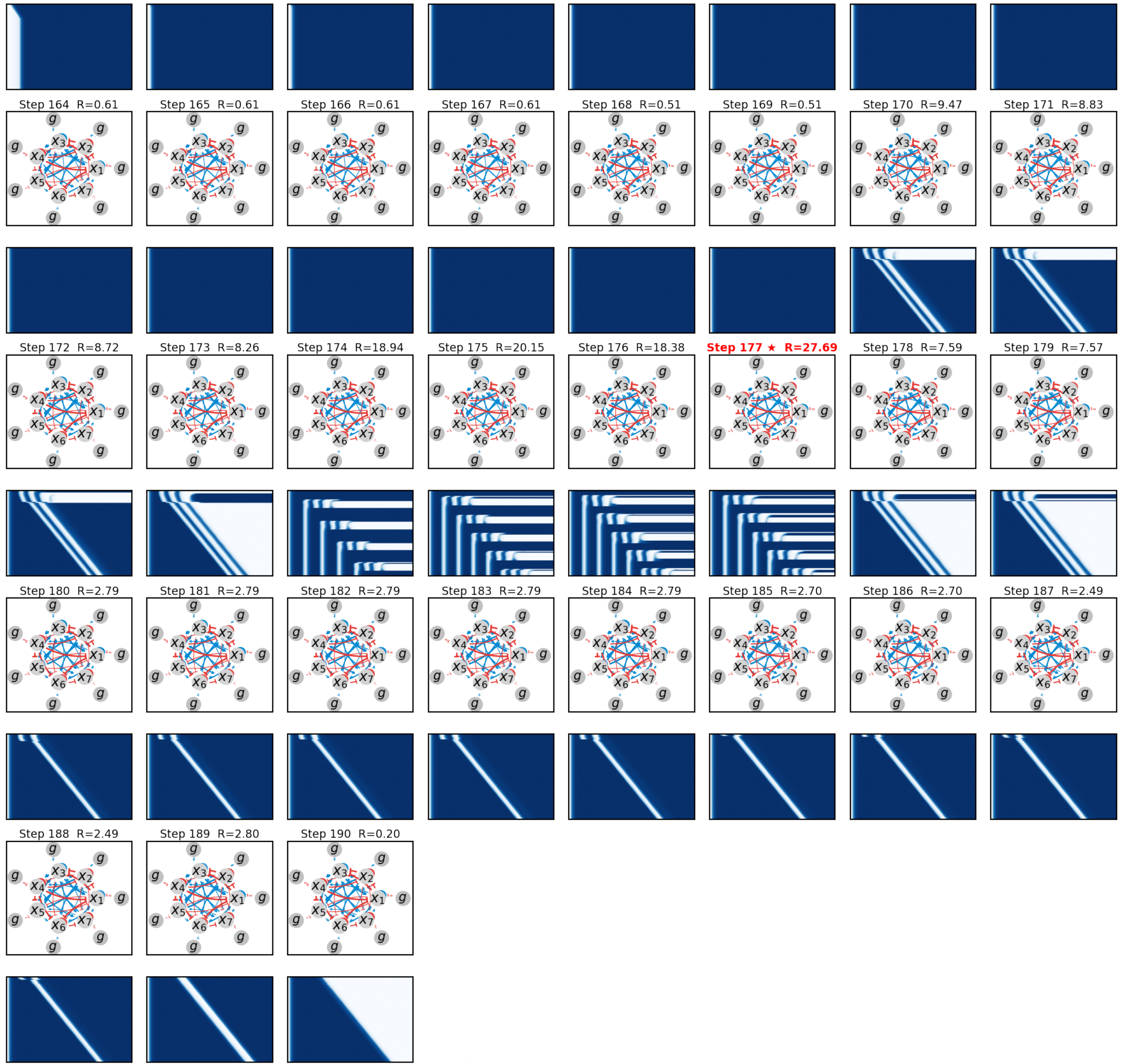
Step 164 R=0.61
Step 165 R=0.61
Step 166 R=0.61
Step 167 R=0.61
Step 168 R=0.51
Step 169 R=0.51
Step 170 R=9.47
Step 171 R=8.83
Step 172 R=8.72
Step 173 R=8.26
Step 174 R=18.94
Step 175 R=20.15
Step 176 R=18.38
Step 177 ★ R=27.69
Step 178 R=7.59
Step 179 R=7.57
Step 180 R=2.79
Step 181 R=2.79
Step 182 R=2.79
Step 183 R=2.79
Step 184 R=2.79
Step 185 R=2.70
Step 186 R=2.70
Step 187 R=2.49
Step 188 R=2.49
Step 189 R=2.80
Step 190 R=0.20
$x_1$
$x_2$
$x_3$
$x_4$
$x_5$
$x_6$
$x_7$
g

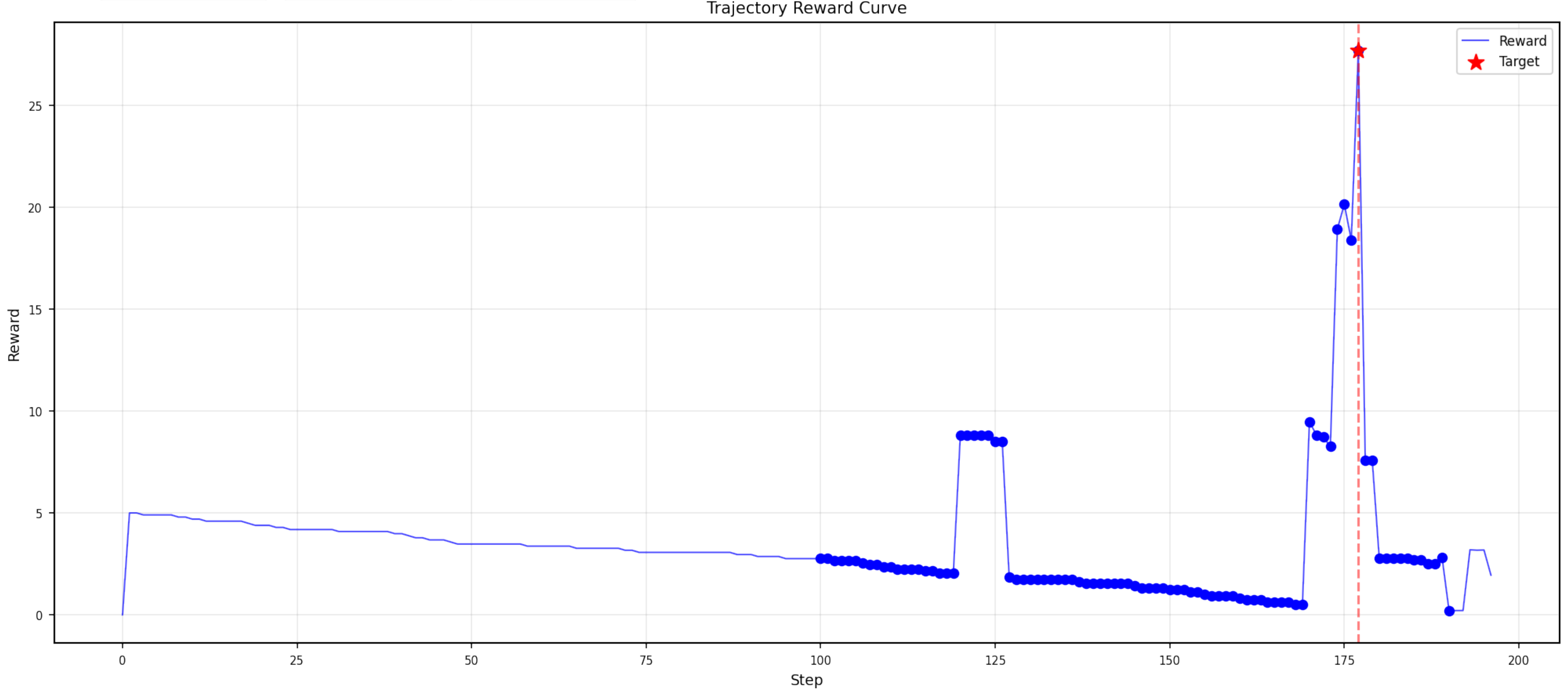
Trajectory Reward Curve
Reward
Target
Reward
Step
0
5
10
15
20
25
0
25
50
75
100
125
150
175
200

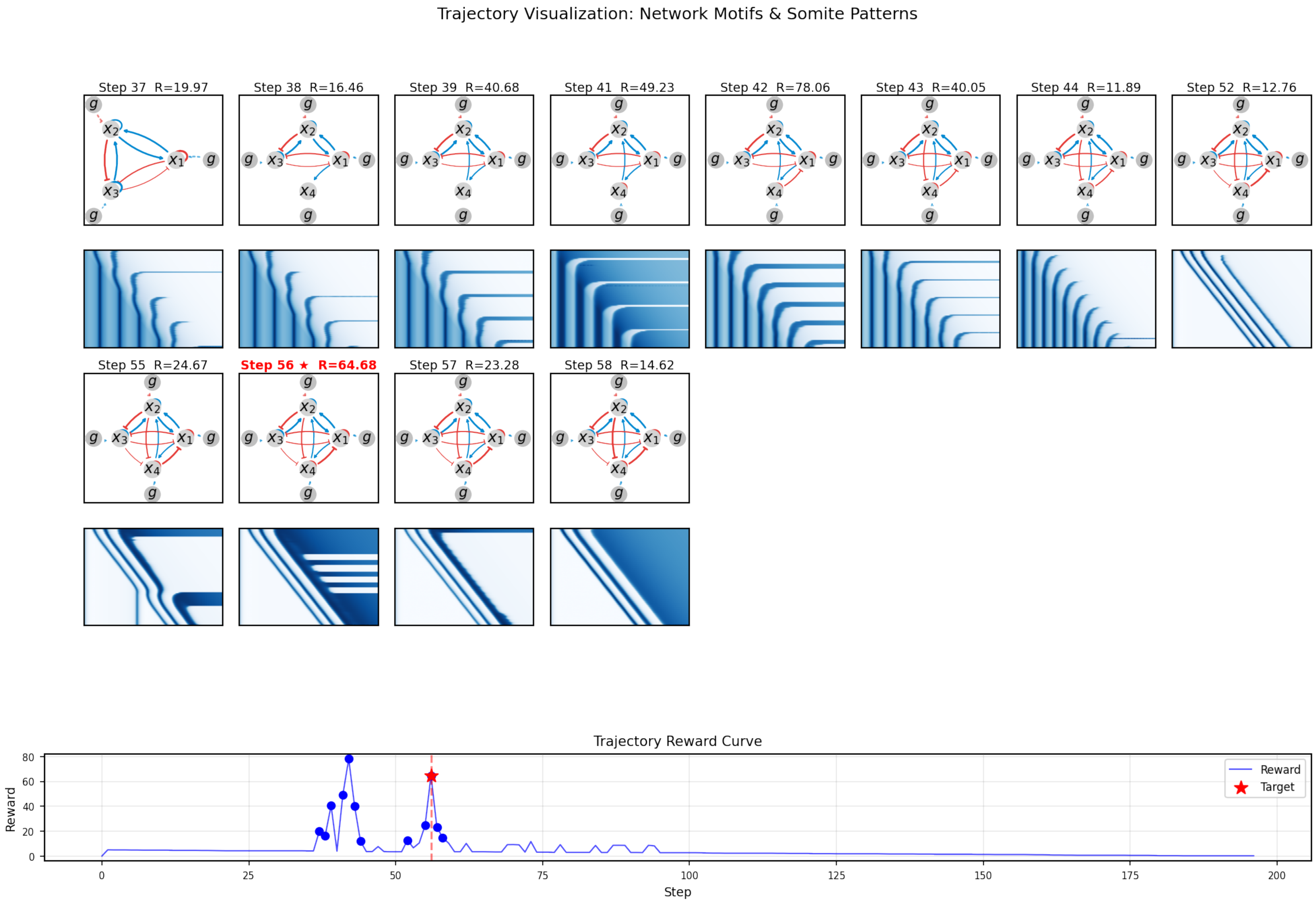
Trajectory Visualization: Network Motifs & Somite Patterns
Step 37 R=19.97
Step 38 R=16.46
Step 39 R=40.68
Step 41 R=49.23
Step 42 R=78.06
Step 43 R=40.05
Step 44 R=11.89
Step 52 R=12.76
Step 55 R=24.67
Step 56 ★ R=64.68
Step 57 R=23.28
Step 58 R=14.62
g
$x_1$
$x_2$
$x_3$
$x_4$
Trajectory Reward Curve
Reward
Step
0
20
40
60
80
0
25
50
75
100
125
150
175
200
Reward
Target

## Trajectory Visualization: Network Motifs & Somite Patterns

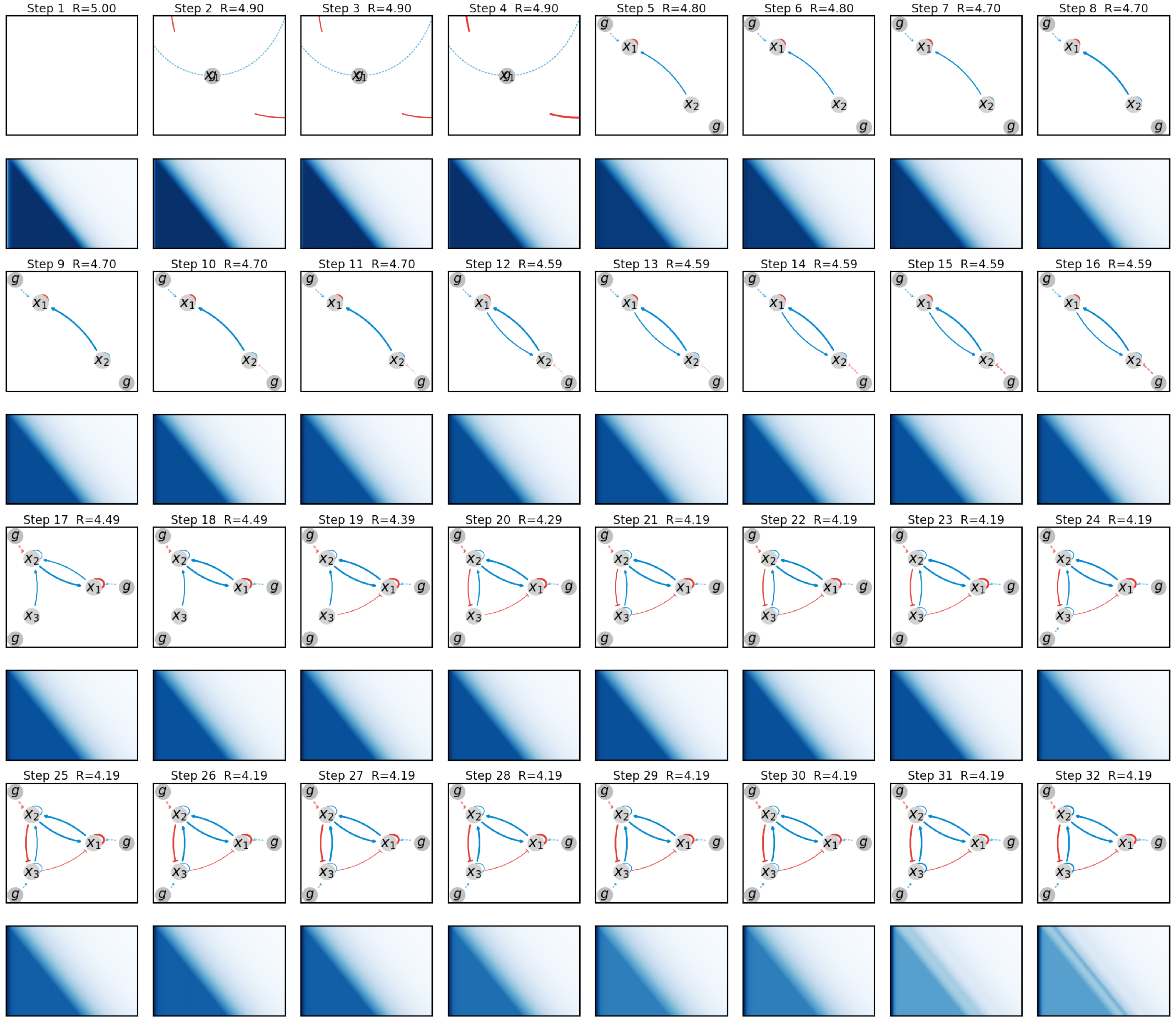

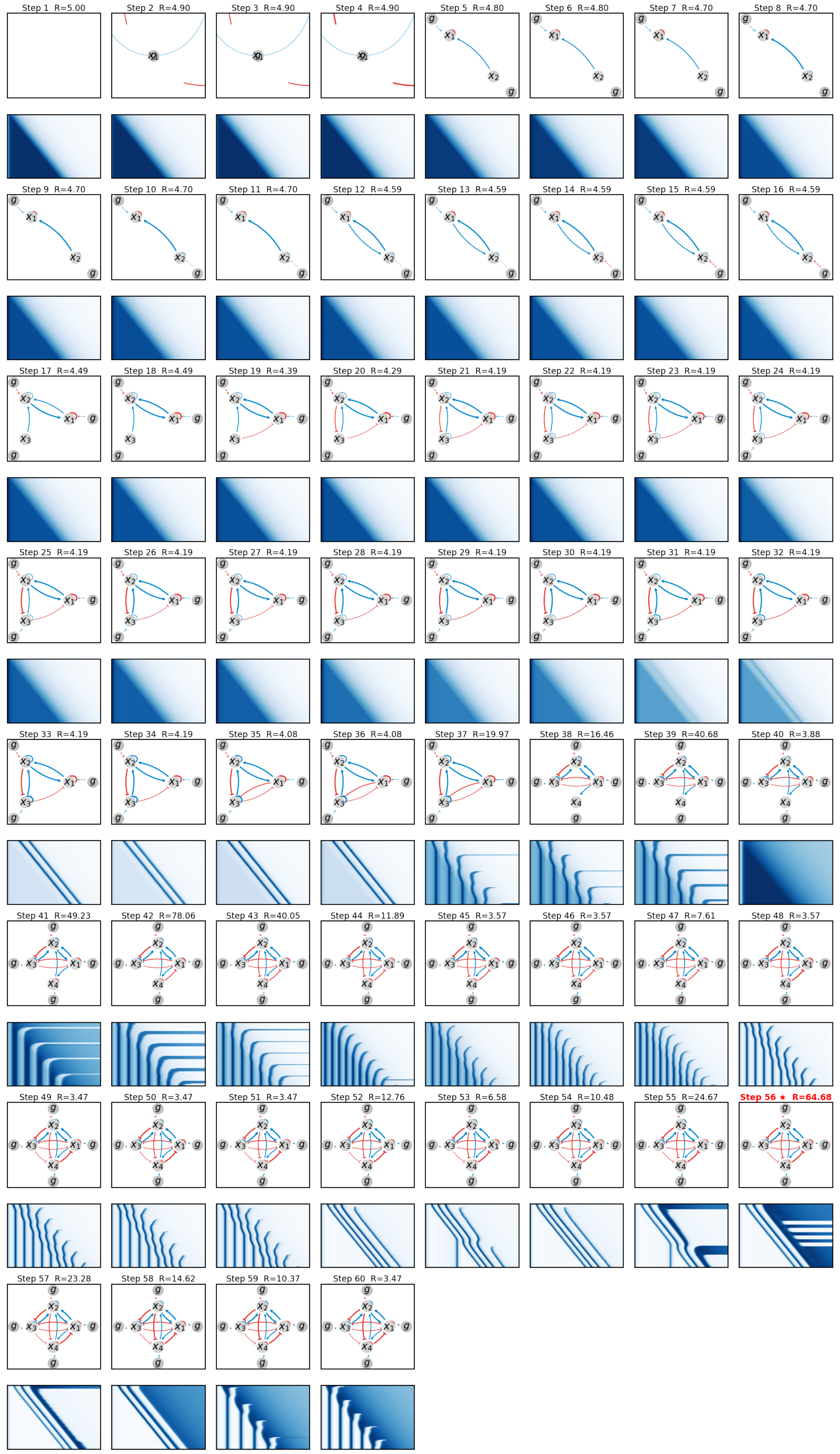

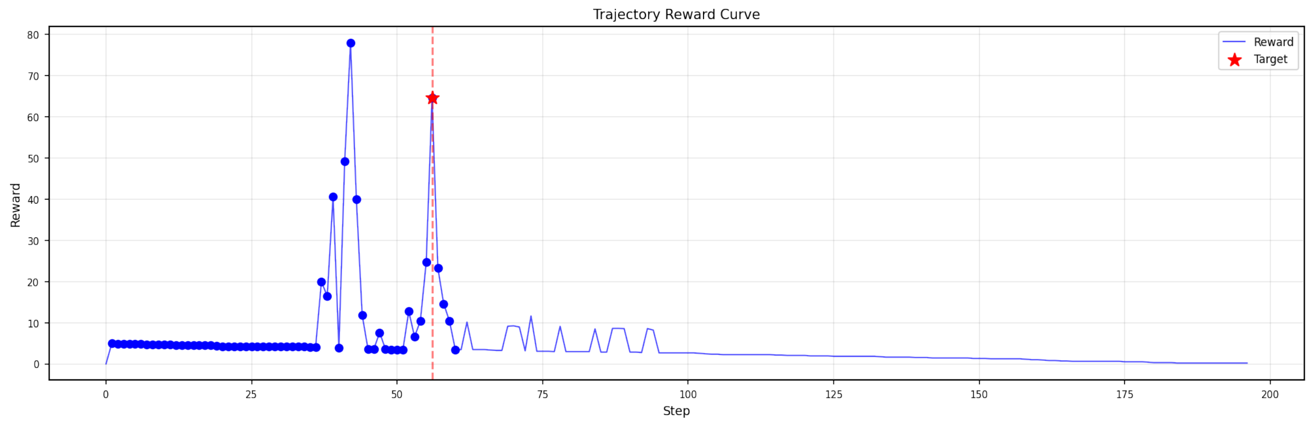

Step 100 R=2.55
Step 101 R=2.55
Step 102 R=2.55
Step 103 R=2.55
Step 104 R=2.45
Step 105 R=2.35
Step 106 R=2.35
Step 107 R=2.35
Step 108 R=2.25
Step 109 R=2.25
Step 110 R=2.14
Step 111 R=2.04
Step 112 R=1.94
Step 113 R=30.15
Step 114 R=16.75
Step 115 R=16.75
Step 116 R=11.26
Step 117 R=38.45
Step 118 R=16.18
Step 119 R=10.75
Step 120 R=1.74
Step 121 R=1.74
Step 122 R=1.74
Step 123 R=1.74
Step 124 R=1.74
Step 125 R=7.44
Step 126 R=7.40
Step 127 R=15.03
Step 128 R=10.02
Step 129 R=1.74
Step 130 R=12.55
Step 131 R=13.33
$x_1$
$x_2$
$x_3$
$x_4$
$x_5$
$x_6$
$g$

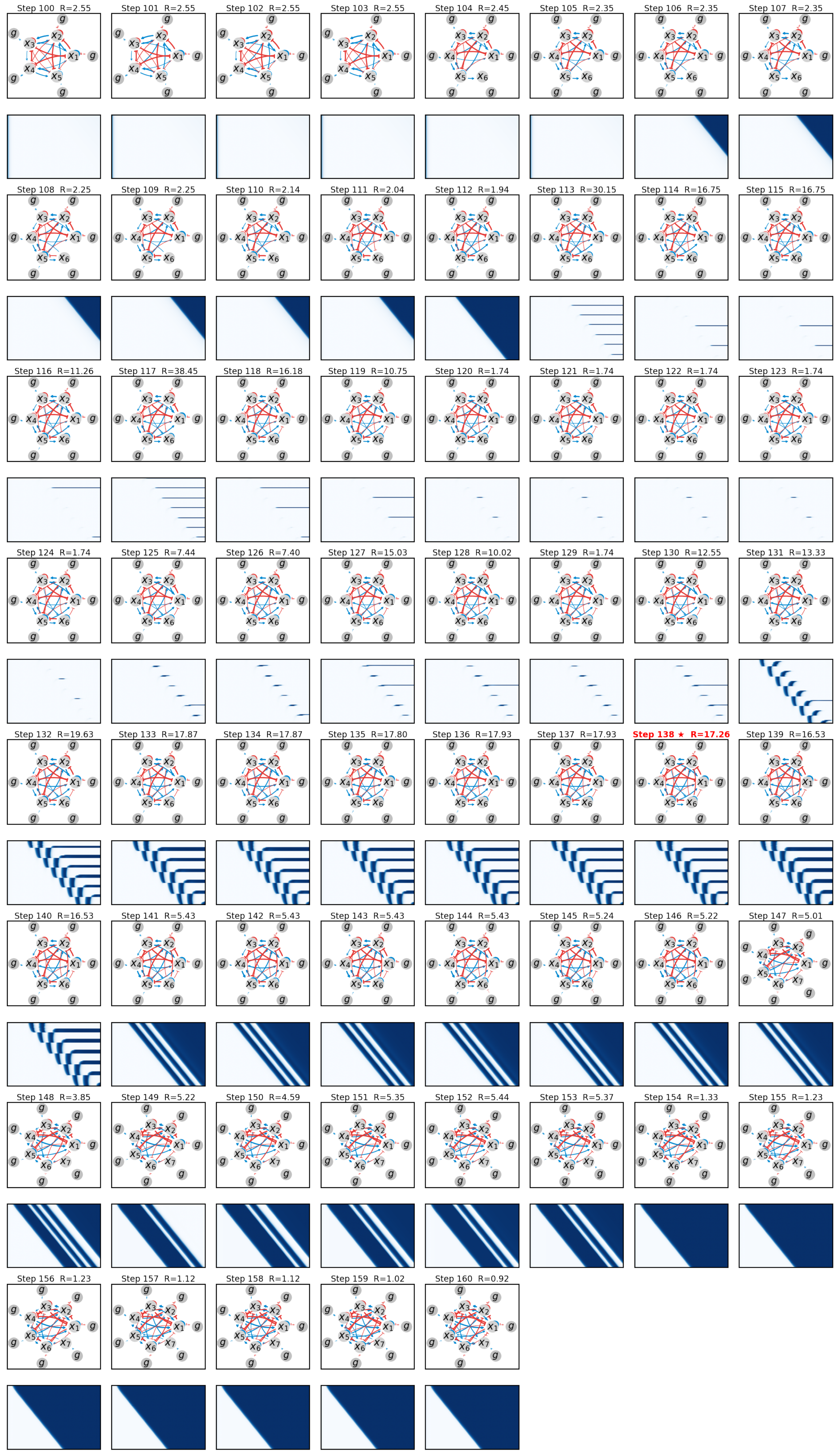

Step 100 R=2.55
Step 101 R=2.55
Step 102 R=2.55
Step 103 R=2.55
Step 104 R=2.45
Step 105 R=2.35
Step 106 R=2.35
Step 107 R=2.35
Step 108 R=2.25
Step 109 R=2.25
Step 110 R=2.14
Step 111 R=2.04
Step 112 R=1.94
Step 113 R=30.15
Step 114 R=16.75
Step 115 R=16.75
Step 116 R=11.26
Step 117 R=38.45
Step 118 R=16.18
Step 119 R=10.75
Step 120 R=1.74
Step 121 R=1.74
Step 122 R=1.74
Step 123 R=1.74
Step 124 R=1.74
Step 125 R=7.44
Step 126 R=7.40
Step 127 R=15.03
Step 128 R=10.02
Step 129 R=1.74
Step 130 R=12.55
Step 131 R=13.33
Step 132 R=19.63
Step 133 R=17.87
Step 134 R=17.87
Step 135 R=17.80
Step 136 R=17.93
Step 137 R=17.93
Step 138 ★ R=17.26
Step 139 R=16.53
Step 140 R=16.53
Step 141 R=5.43
Step 142 R=5.43
Step 143 R=5.43
Step 144 R=5.43
Step 145 R=5.24
Step 146 R=5.22
Step 147 R=5.01
Step 148 R=3.85
Step 149 R=5.22
Step 150 R=4.59
Step 151 R=5.35
Step 152 R=5.44
Step 153 R=5.37
Step 154 R=1.33
Step 155 R=1.23
Step 156 R=1.23
Step 157 R=1.12
Step 158 R=1.12
Step 159 R=1.02
Step 160 R=0.92
$x_1$
$x_2$
$x_3$
$x_4$
$x_5$
$x_6$
$x_7$
$g$

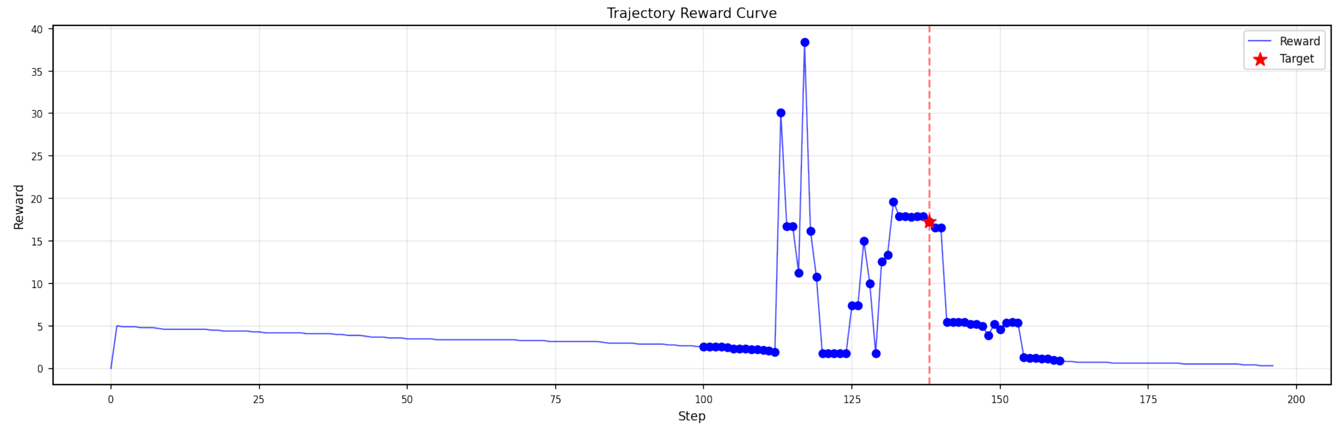

Trajectory Reward Curve
Reward
Step
0
5
10
15
20
25
30
35
40
0
25
50
75
100
125
150
175
200
Reward
Target

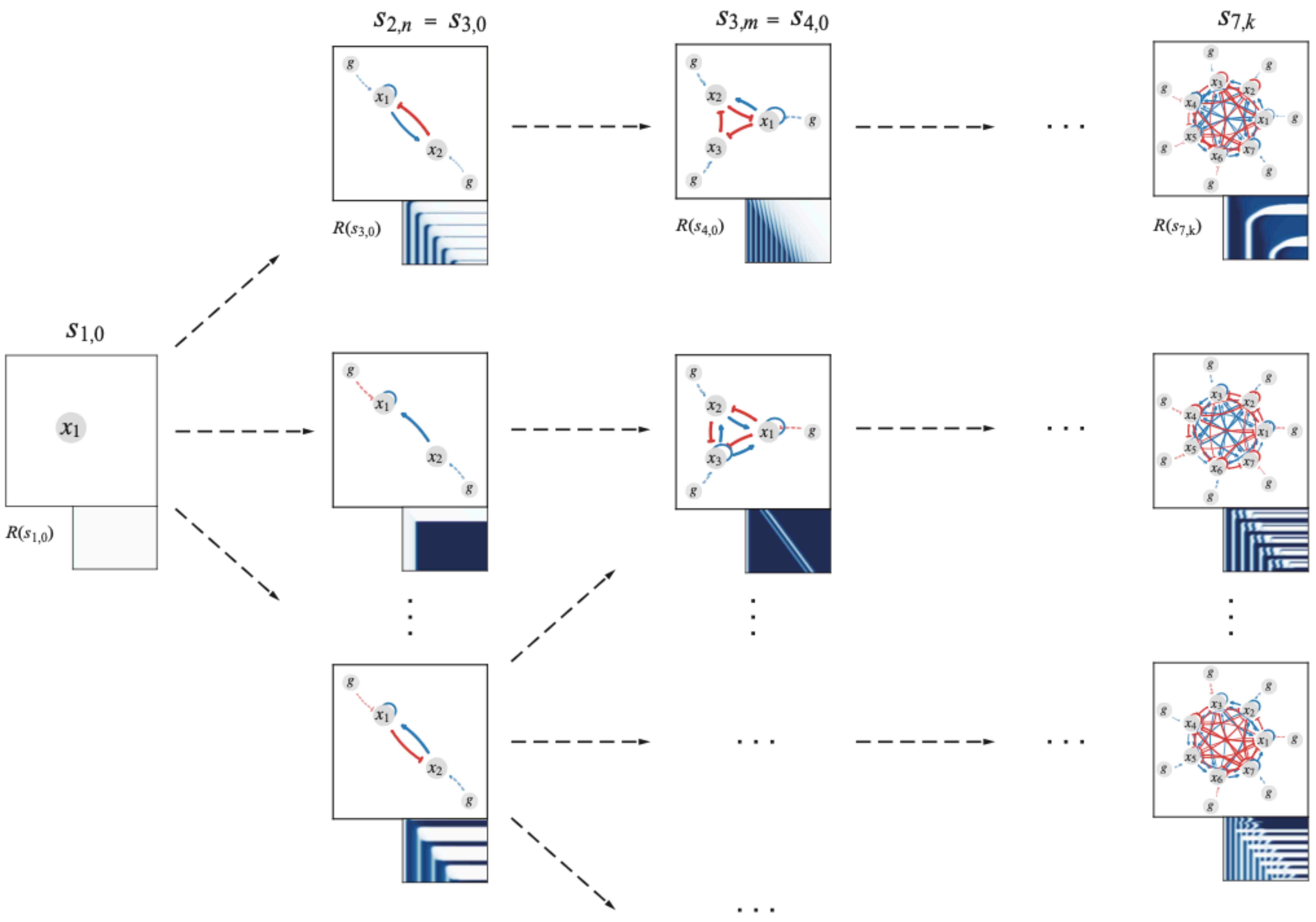

Figure 1: Illustration of the node-first search strategy. For a fixed number of nodes $i$, the GFlowNet updates edges within the subnetwork along a trajectory $s_{i,0} \to \cdots \to s_{i,T_i}$. When the subnetwork is explored, a new node is added and the search continues from $s_{i+1,0}$ with $s_{i,T_i} = s_{i+1,0}$. Each state is a motif and the reward $R(s_{i,k})$ computed from the simulated kymograph.

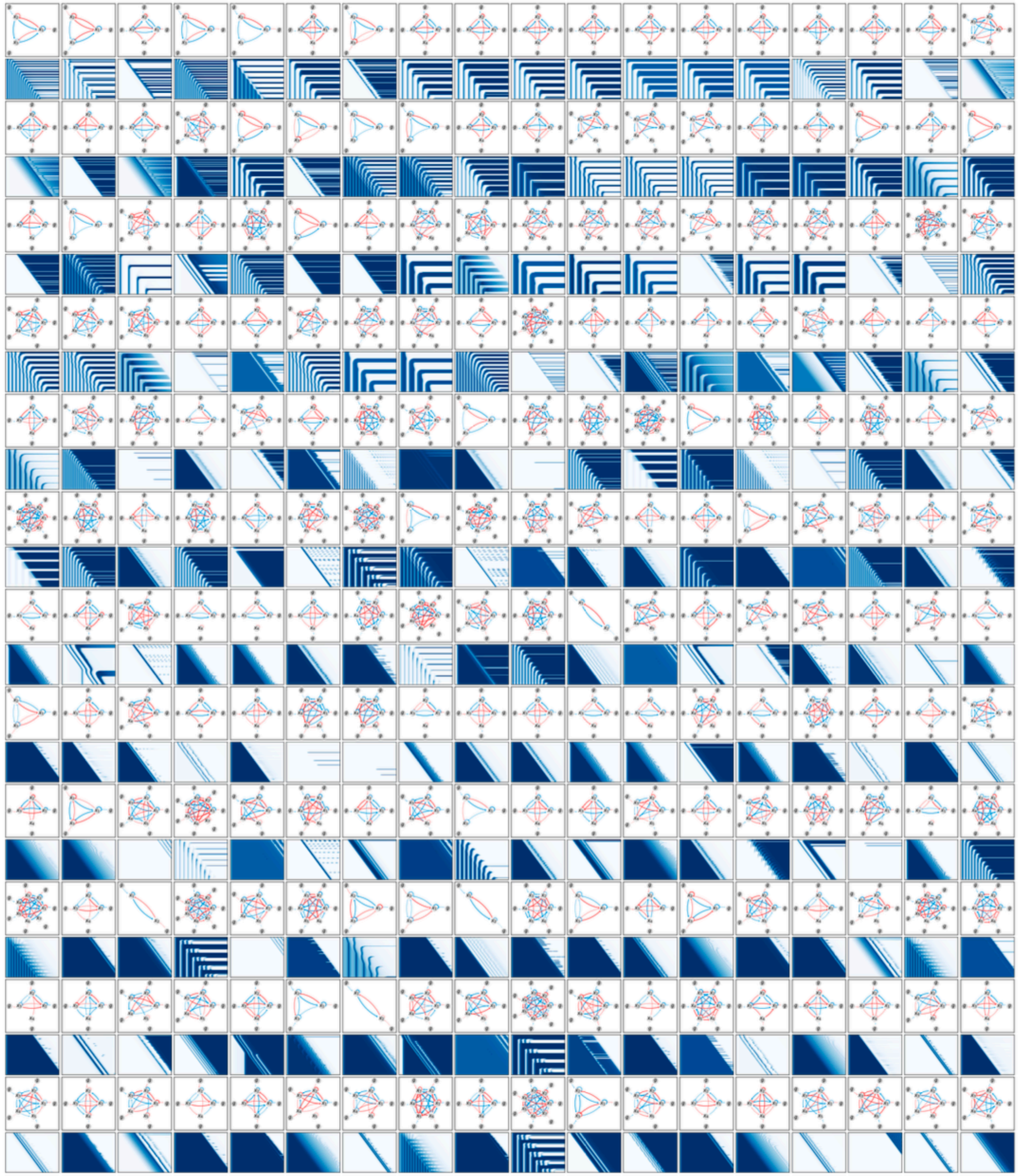

Figure 2: Top high-reward modes discovered in a single GFlowNet run on the somitogenesis task. Each grid displays a distinct solution, illustrating the underlying GRN motif and its corresponding kymograph.

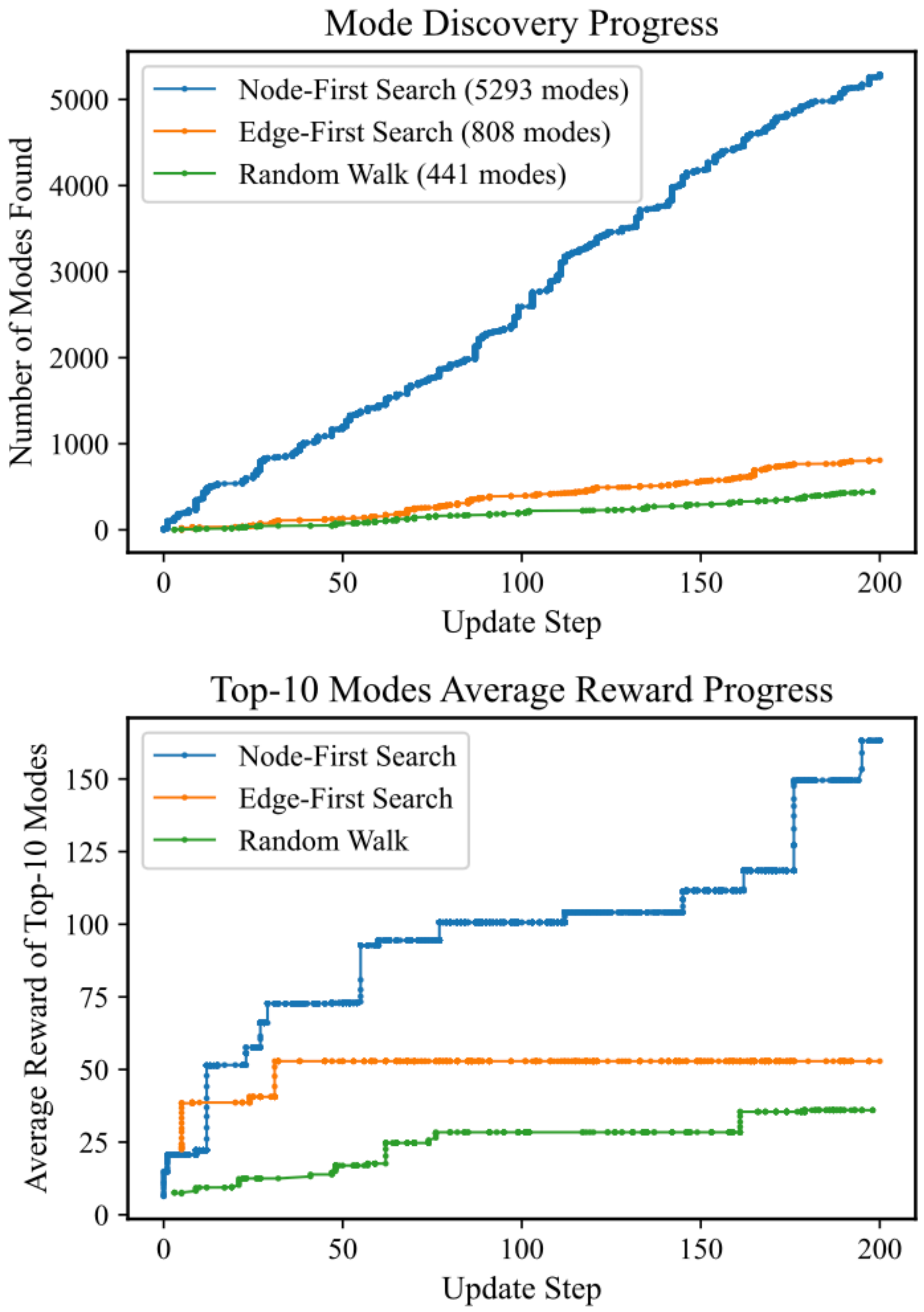

Figure 3: Benchmarks of three search strategies on the somitogenesis task. Top: cumulative number of distinct modes discovered vs. update step. Bottom: average reward of the top-10 modes. “Node-first” outperforms “edge-first” and random walk on both metrics.

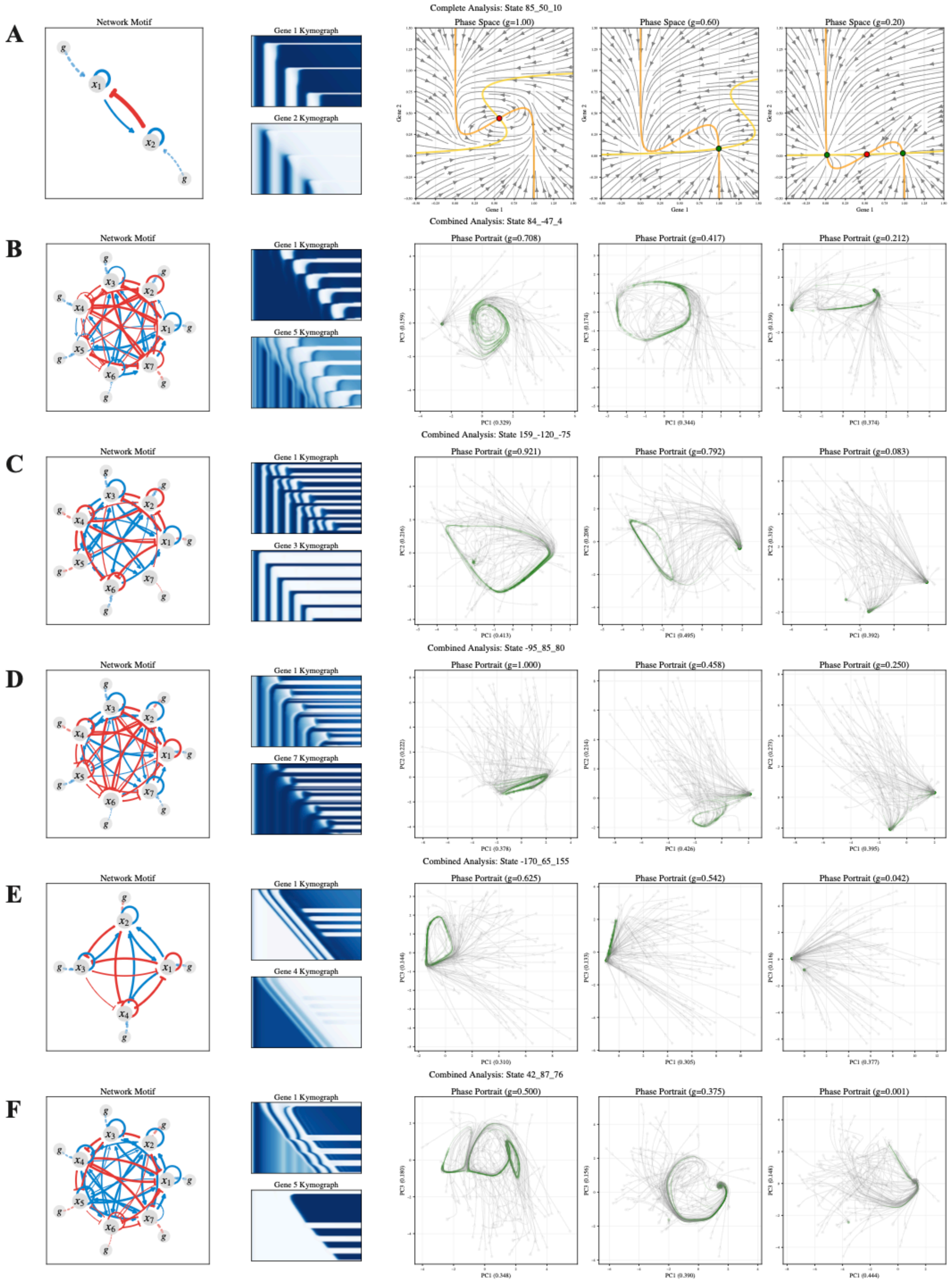

Figure 4: Analysis of some unexpected modes discovered by the GFlowNet with 'node-first' searhcing strategy. Columns (left to right): generated GRN motif; kymographs of selected genes; phase portraits/phase space as the morphogen level $g$ decreases. Trajectories highlight attractors (fixed points or limit cycles) and how they evolve with control parameter $g$.

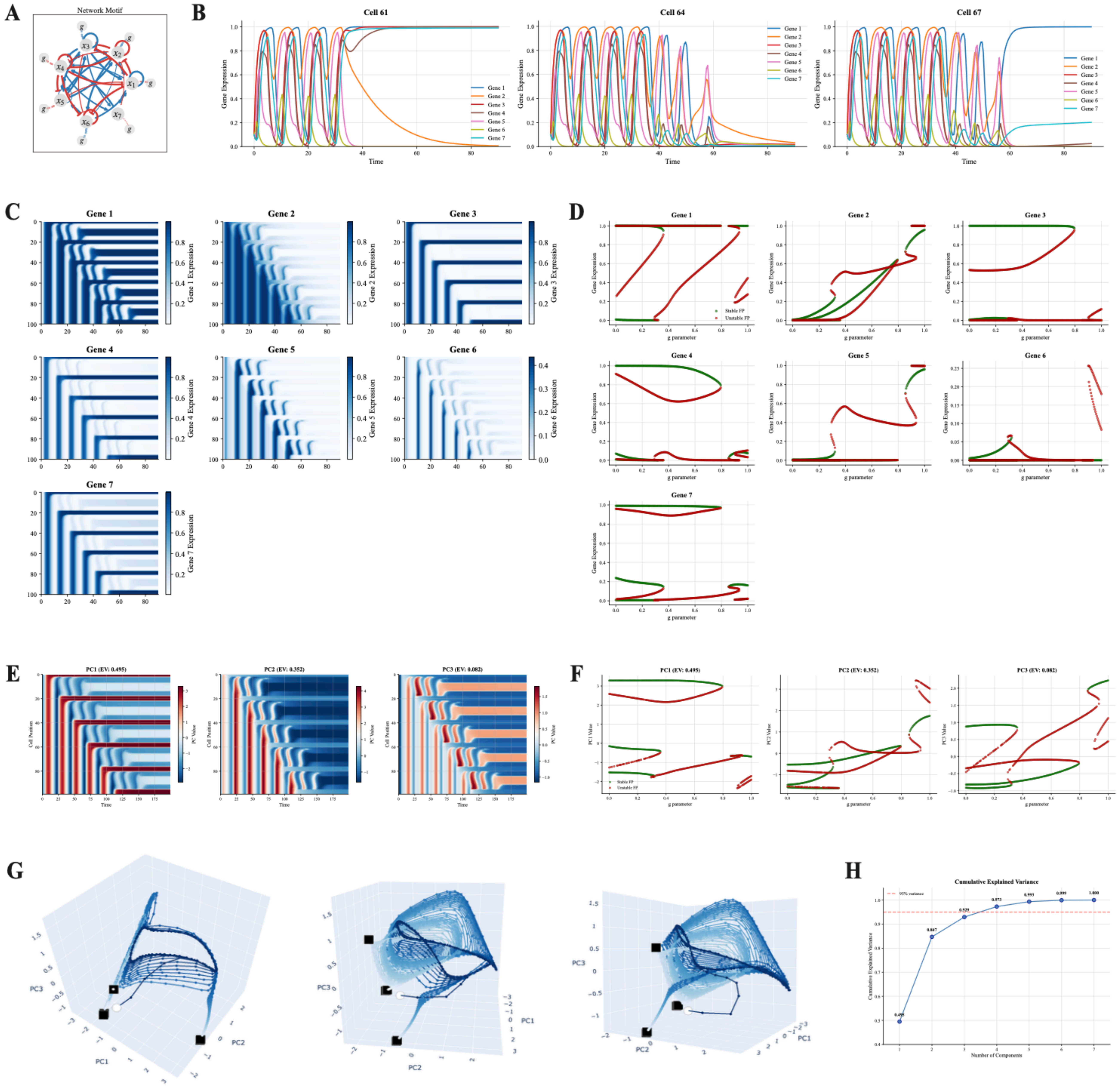

Figure 7: state analysis.

But How to model GRN really ?

TABLE 1. SUMMARY OF PROPERTIES OF DIFFERENT MODELING FORMALISMS: DIRECTED GRAPHS (DG), BAYESIAN NETWORKS (BYN), BOOLEAN NETWORKS (BNN), GENERALIZED LOGICAL NETWORKS (GLN), NONLINEAR DIFFERENTIAL EQUATIONS (NLDE), PIECEWISE-LINEAR DIFFERENTIAL EQUATIONS (PLDE), PARTIAL DIFFERENTIAL EQUATIONS (PDE), STOCHASTIC MASTER EQUATIONS (SME), AND RULE-BASE FORMALISMS (R)

| | *Static (s), dynamic (d)* | *Discrete (d), continuous (c)* | *Deterministic (d), stochastic (s)* | *Qualitative (ql), quantitative (qn)* | *Coarse (c), average (a), fine (f) grained* |
|---|---|---|---|---|---|
| DG | s | | d | ql | c |
| BYN | s[a] | d,c | s | qn | c |
| BNN | d | d | d | ql | c |
| GLN | d | d | d | ql | a |
| NLDE | d | c | d | qn | a,f |
| PLDE | d | c | d | ql,qn[c] | a |
| QDE | d | d | d | ql | a,f |
| SDE? PDE | d | c[b] | d | qn | a,f |
| SME | d | d | s | qn | f |
| R | d | d | d | ql | a,f |

[a] Generalization to dynamic Boolean networks is possible.

[b] Spatial dimension is often discretized.

[c] Qualitative analysis of models is possible.

DE vs. ME

H. de Jong, J. Comput. Biol., 9(1), 2002.

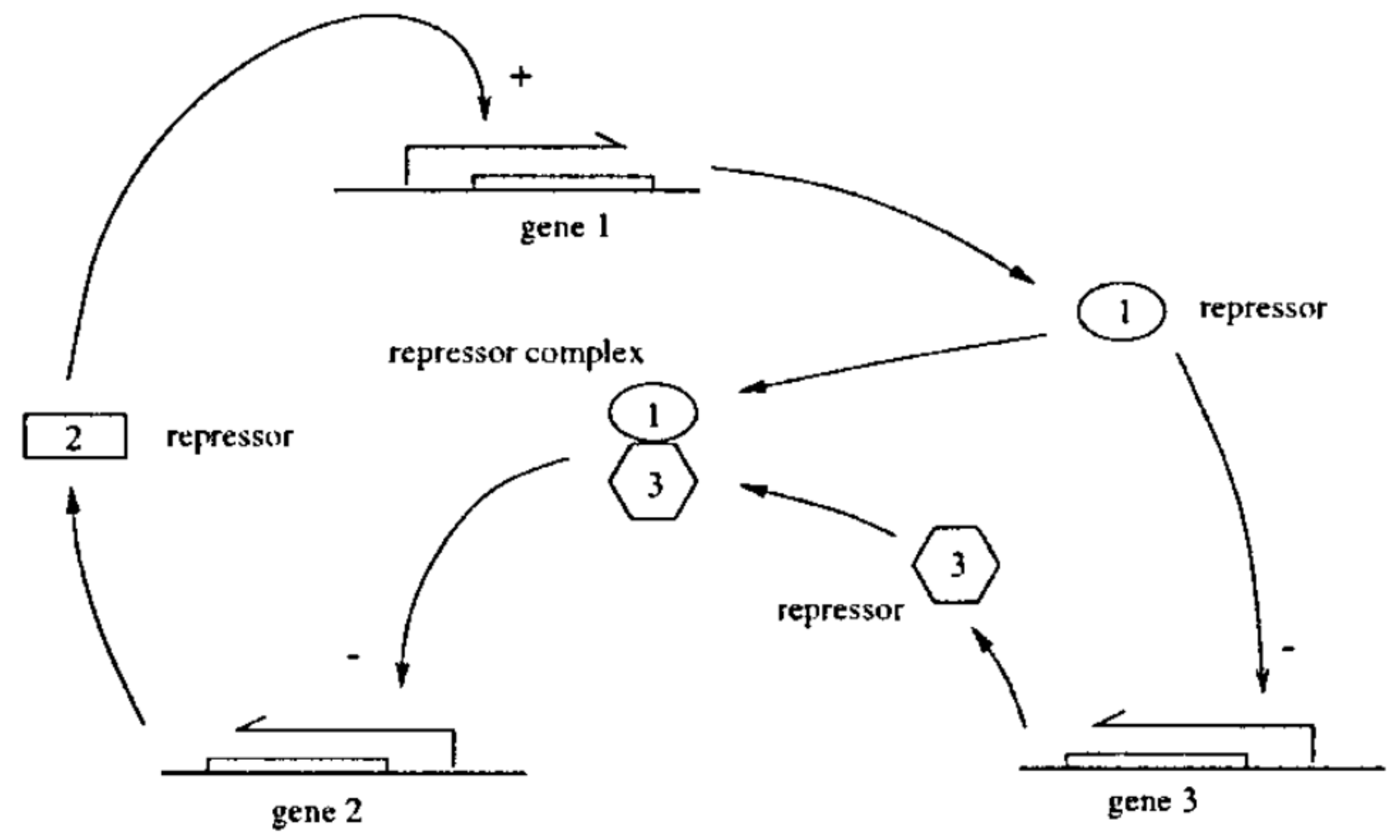

(a)

$$\dot{x}_1 = \kappa_1\, s^+(x_2, \theta_{21}) - \gamma_1\, x_1$$
$$\dot{x}_2 = \kappa_2\, (1 - s^+(x_1, \theta_{11})\, s^+(x_3, \theta_{31})) - \gamma_2\, x_2$$
$$\dot{x}_3 = \kappa_3\, s^-(x_1, \theta_{12}) + \kappa_4\, s^-(x_3, \theta_{32}) - \gamma_3\, x_3$$

(b)

**FIG. 9.** **(a)** Example regulatory network of three genes and **(b)** corresponding piecewise-linear differential equations; $x_1$, $x_2$, and $x_3$ represent protein or mRNA concentrations, respectively, $\kappa_1, \ldots, \kappa_4$ production constants, $\gamma_1, \ldots, \gamma_3$ degradation constants, and $\theta_{11}, \theta_{12}, \theta_{21}, \theta_{31}, \theta_{32}$ threshold constants.

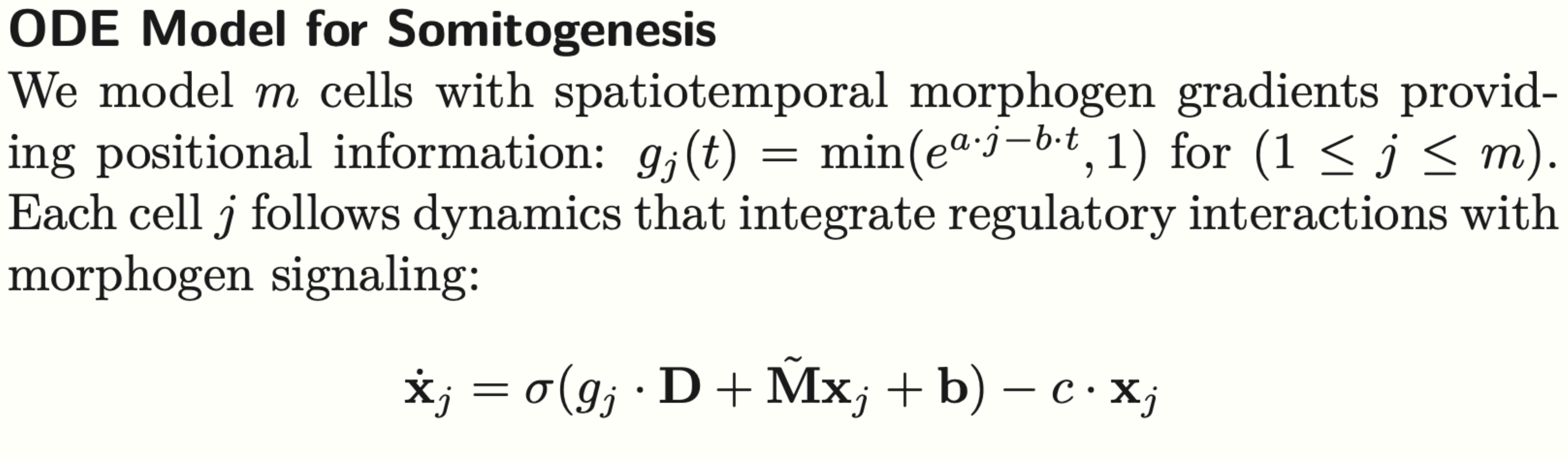

## ODE Model for Somitogenesis

We model $m$ cells with spatiotemporal morphogen gradients providing positional information: $g_j(t) = \min(e^{a \cdot j - b \cdot t}, 1)$ for $(1 \leq j \leq m)$. Each cell $j$ follows dynamics that integrate regulatory interactions with morphogen signaling:

$$\dot{\mathbf{x}}_j = \sigma(g_j \cdot \mathbf{D} + \tilde{\mathbf{M}}\mathbf{x}_j + \mathbf{b}) - c \cdot \mathbf{x}_j$$

# Segmentation Networks

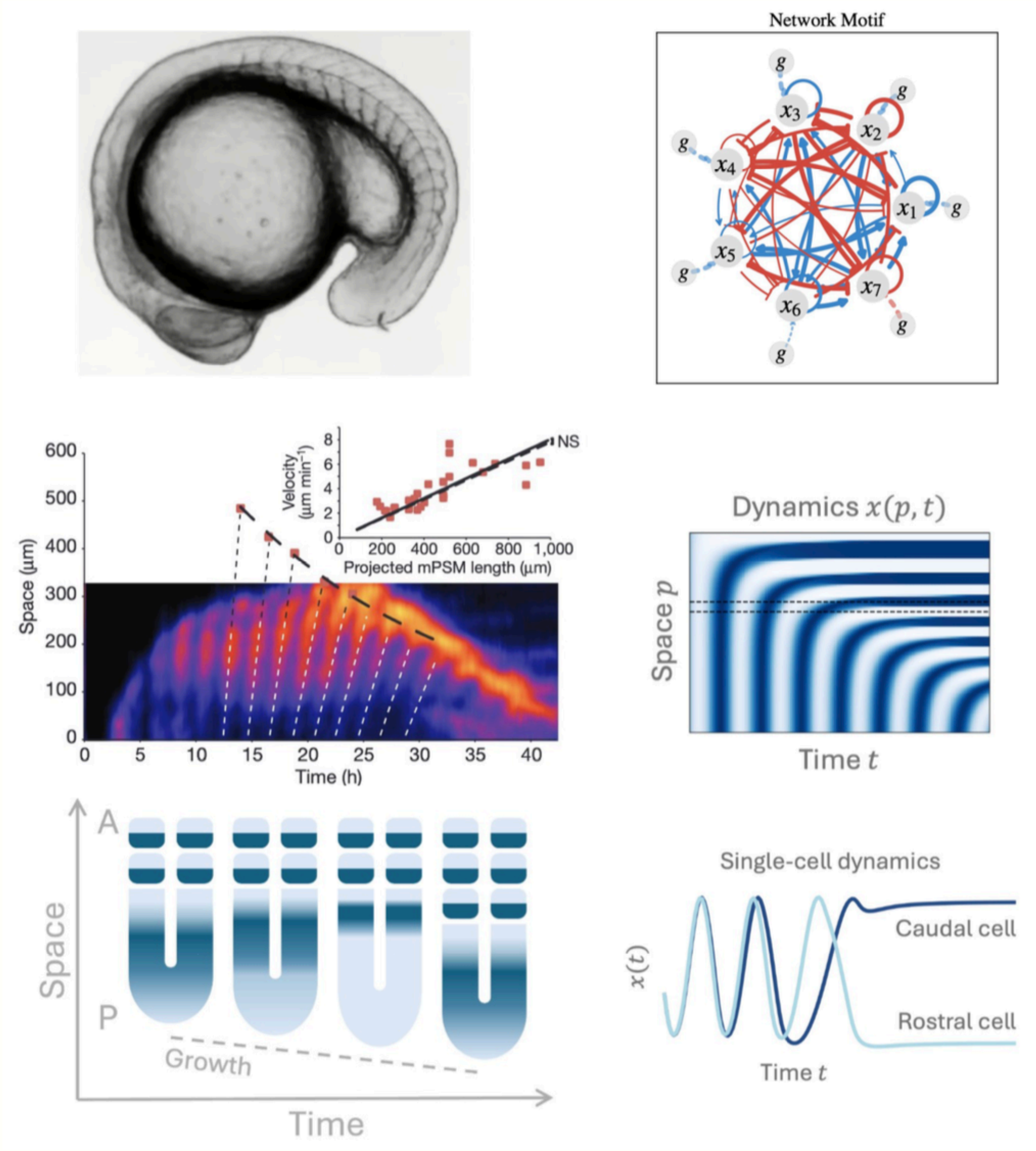

## ODE Model for Somitogenesis

We model $m$ cells with spatiotemporal morphogen gradients providing positional information: $g_j(t) = \min(e^{a\cdot j - b\cdot t}, 1)$ for $(1 \leq j \leq m)$. Each cell $j$ follows dynamics that integrate regulatory interactions with morphogen signaling:

$$\dot{\mathbf{x}}_j = \sigma(g_j \cdot \mathbf{D} + \tilde{\mathbf{M}}\mathbf{x}_j + \mathbf{b}) - c \cdot \mathbf{x}_j$$

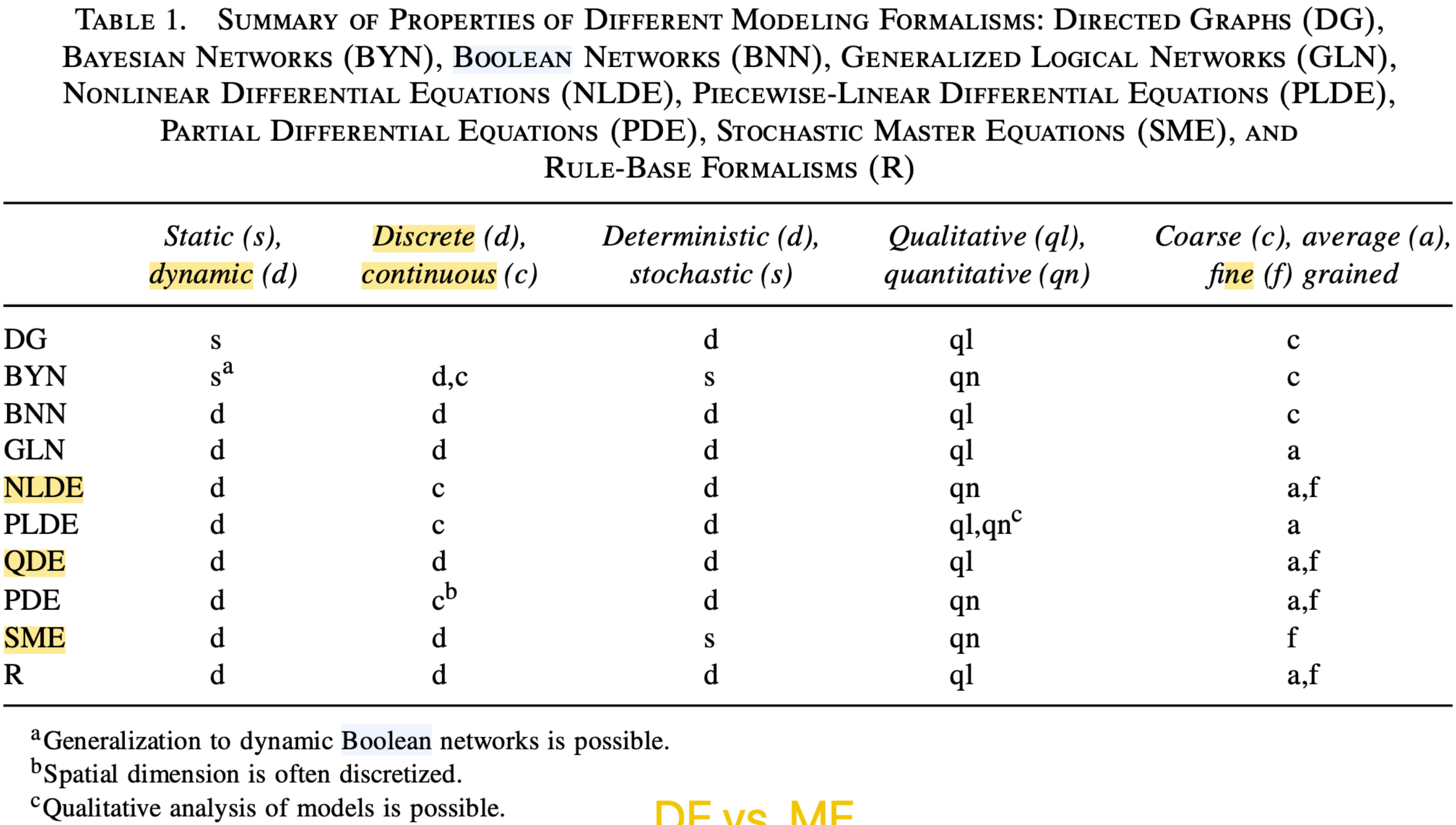

Table 1. Summary of Properties of Different Modeling Formalisms: Directed Graphs (DG), Bayesian Networks (BYN), Boolean Networks (BNN), Generalized Logical Networks (GLN), Nonlinear Differential Equations (NLDE), Piecewise-Linear Differential Equations (PLDE), Partial Differential Equations (PDE), Stochastic Master Equations (SME), and Rule-Base Formalisms (R)

| | *Static (s), dynamic (d)* | *Discrete (d), continuous (c)* | *Deterministic (d), stochastic (s)* | *Qualitative (ql), quantitative (qn)* | *Coarse (c), average (a), fine (f) grained* |
|---|---|---|---|---|---|
| DG | s | | d | ql | c |
| BYN | s[a] | d,c | s | qn | c |
| BNN | d | d | d | ql | c |
| GLN | d | d | d | ql | a |
| NLDE | d | c | d | qn | a,f |
| PLDE | d | c | d | ql,qn[c] | a |
| QDE | d | d | d | ql | a,f |
| PDE | d | c[b] | d | qn | a,f |
| SME | d | d | s | qn | f |
| R | d | d | d | ql | a,f |

[a] Generalization to dynamic Boolean networks is possible.

[b] Spatial dimension is often discretized.

[c] Qualitative analysis of models is possible.

SDE?

DE vs. ME

H. de Jong, J. Comput. Biol., 9(1), 2002.

# SDE model

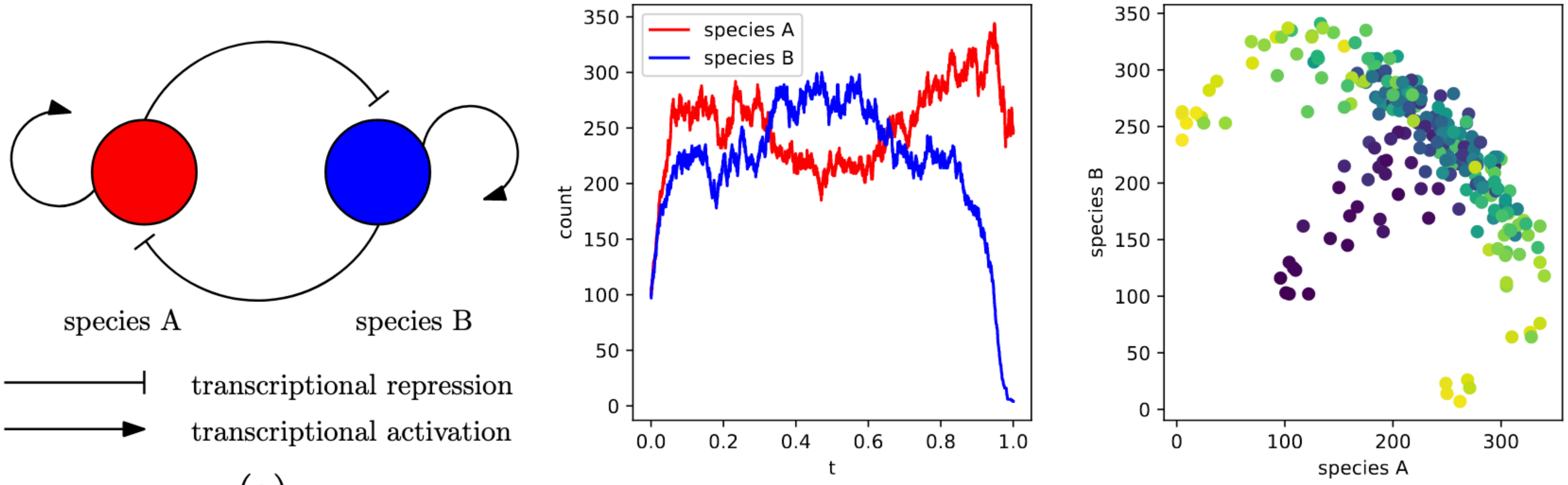

(a)

(b)

(c)

Figure 1.3: (a) Bistable gene regulatory network comprised of two mutually repressive species (b) Example molecular trajectory (c) Sampled states over bifurcating process, coloured by simulation time $t$.

S. Y. Zhang, MSc Thesis, Univ. Melbourne, 2019.

For brevity, let us write $p(x,t|x_0,t_0) = \mathbf{P}[X_t = x|x_0,t_0]$. Then, in the interval $[t, t+\mathrm{d}t)$, an inflow-outflow argument gives us the chemical master equation:

$$\frac{\partial p(x,t|x_0,t_0)}{\partial t} = \sum_{j=1}^{M} \left[ f_j(x - \Delta X_j) p(x - \Delta X_j, t|x_0,t_0) - f_j(x) p(x,t|x_0,t_0) \right],$$

The CME describes the evolution of $p(x,t|x_0,t_0)$ in $t$ as a set of coupled ODEs, one for each possible configuration state $X = x$. We can view the CME as assigning some probability density to every possible trajectory in the finite state space. Because of the discrete setting, the space of possible configurations is finite but possibly very large. The CME is therefore difficult to solve exactly for all but the simplest reaction networks, and the typical approach is to resort to sampling. To this end, Gillespie's algorithm is a very well known Monte-Carlo sampling scheme for the CME. In essence, Gillespie [61, Section 2] shows that the evolution of the reaction network can be cast as a continuous-time random walk on the discrete state space with exponential transitions at state-dependent rates, from which a straightforward method for exact sampling can be developed. For the two-species GRN we consider earlier, we show a sample trajectory obtained by the Gillespie algorithm in Figure 1.3(b).

There is a large literature focusing on continuous approximations of the CME in various limiting regimes. Perhaps most notably, in the regime of large numbers of molecular species, passing the system of ODEs to a limit in the state space yields the chemical Langevin equation (CLE) [61]:

$$\mathrm{d}X_t = \sum_{j=1}^{M} \Delta X_j f_j(X_t)\, \mathrm{d}t + \sum_{j=1}^{M} \Delta X_j \sqrt{f_j(X_t)}\, \mathrm{d}B_t.$$

S. Y. Zhang, MSc Thesis, Univ. Melbourne, 2019.

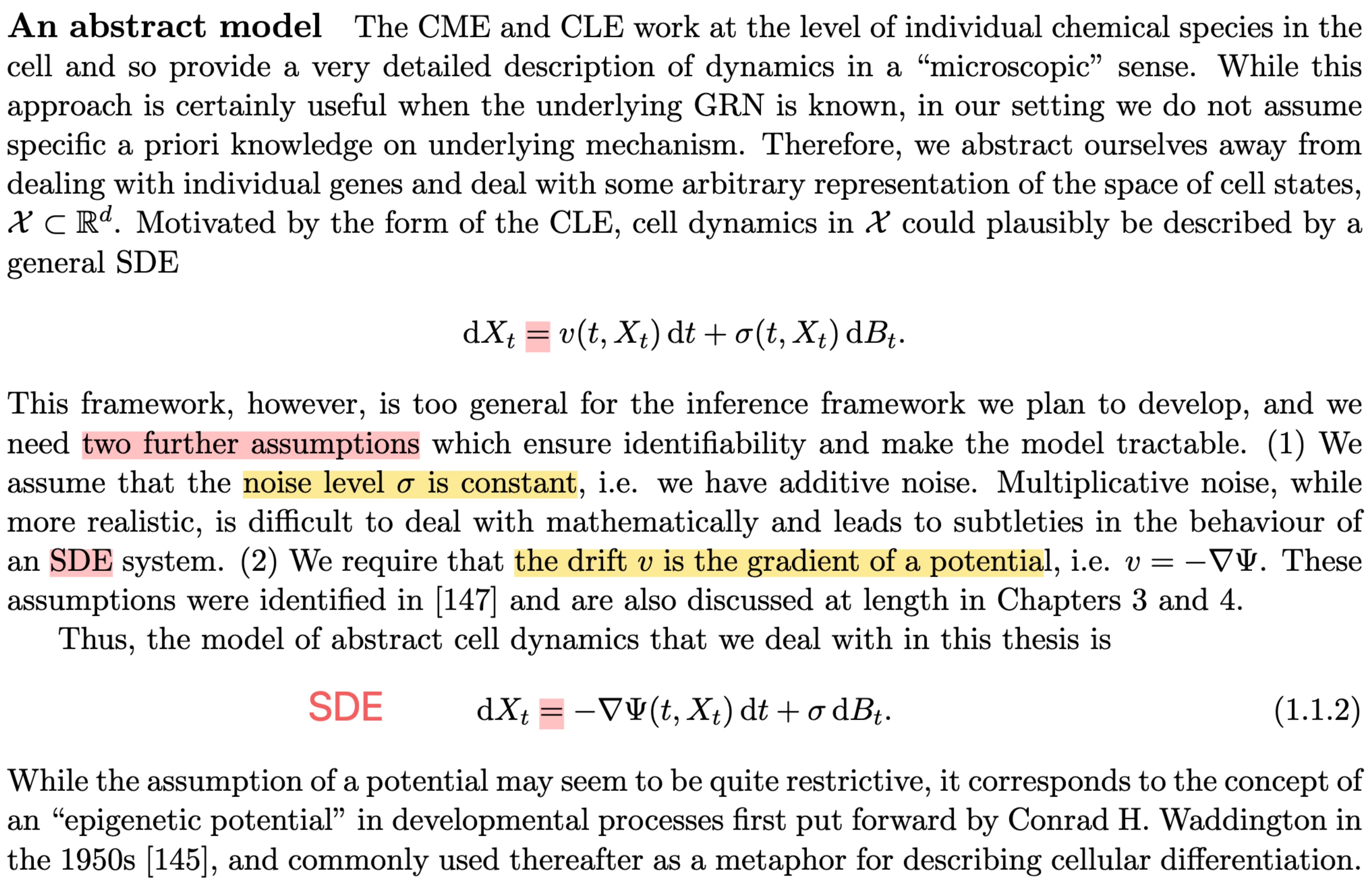

**An abstract model** The CME and CLE work at the level of individual chemical species in the cell and so provide a very detailed description of dynamics in a "microscopic" sense. While this approach is certainly useful when the underlying GRN is known, in our setting we do not assume specific a priori knowledge on underlying mechanism. Therefore, we abstract ourselves away from dealing with individual genes and deal with some arbitrary representation of the space of cell states, $\mathcal{X} \subset \mathbb{R}^d$. Motivated by the form of the CLE, cell dynamics in $\mathcal{X}$ could plausibly be described by a general SDE

$$\mathrm{d}X_t = v(t, X_t)\,\mathrm{d}t + \sigma(t, X_t)\,\mathrm{d}B_t.$$

This framework, however, is too general for the inference framework we plan to develop, and we need two further assumptions which ensure identifiability and make the model tractable. (1) We assume that the noise level $\sigma$ is constant, i.e. we have additive noise. Multiplicative noise, while more realistic, is difficult to deal with mathematically and leads to subtleties in the behaviour of an SDE system. (2) We require that the drift $v$ is the gradient of a potential, i.e. $v = -\nabla\Psi$. These assumptions were identified in [147] and are also discussed at length in Chapters 3 and 4.

Thus, the model of abstract cell dynamics that we deal with in this thesis is

SDE

$$\mathrm{d}X_t = -\nabla\Psi(t, X_t)\,\mathrm{d}t + \sigma\,\mathrm{d}B_t. \qquad (1.1.2)$$

While the assumption of a potential may seem to be quite restrictive, it corresponds to the concept of an "epigenetic potential" in developmental processes first put forward by Conrad H. Waddington in the 1950s [145], and commonly used thereafter as a metaphor for describing cellular differentiation.

S. Y. Zhang, MSc Thesis, Univ. Melbourne, 2019.

**Waddington's epigenetic landscape** Waddington [145] illustrated differentiating cells as marbles rolling down a potential landscape, moving from some initial region of "high developmental potential" and settling in potential wells with "low developmental potential". One can therefore think of the developmental potential as some notion of cell developmental potency. Figure 1.4 shows a conceptual illustration of such a potential landscape.

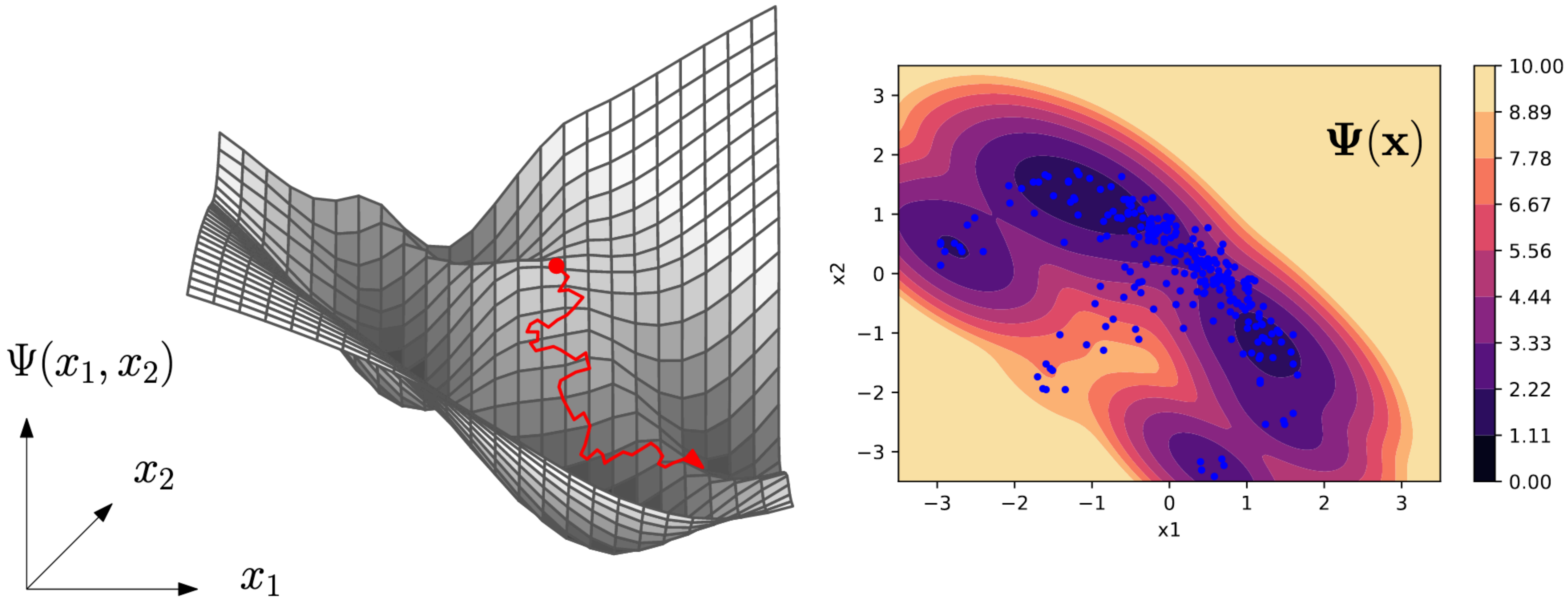

Figure 1.4: The author's impression of "Waddington's epigenetic landscape".

S. Y. Zhang, MSc Thesis, Univ. Melbourne, 2019.

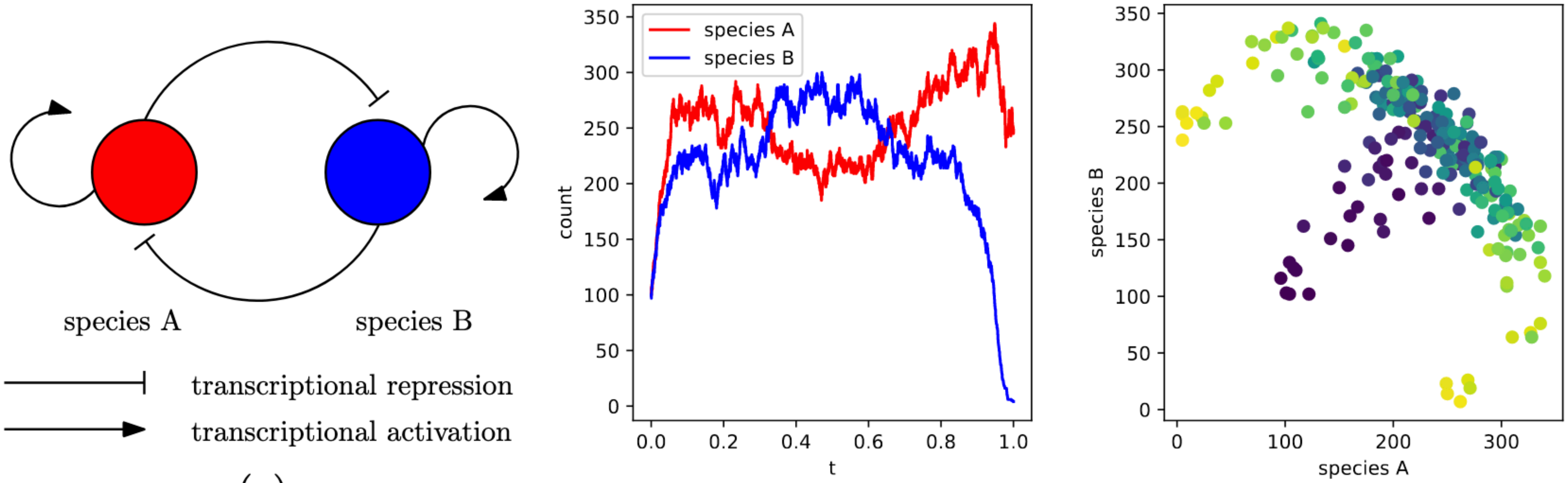

(a)

(b)

(c)

Figure 1.3: (a) Bistable gene regulatory network comprised of two mutually repressive species (b) Example molecular trajectory (c) Sampled states over bifurcating process, coloured by simulation time $t$.

S. Y. Zhang, MSc Thesis, Univ. Melbourne, 2019.

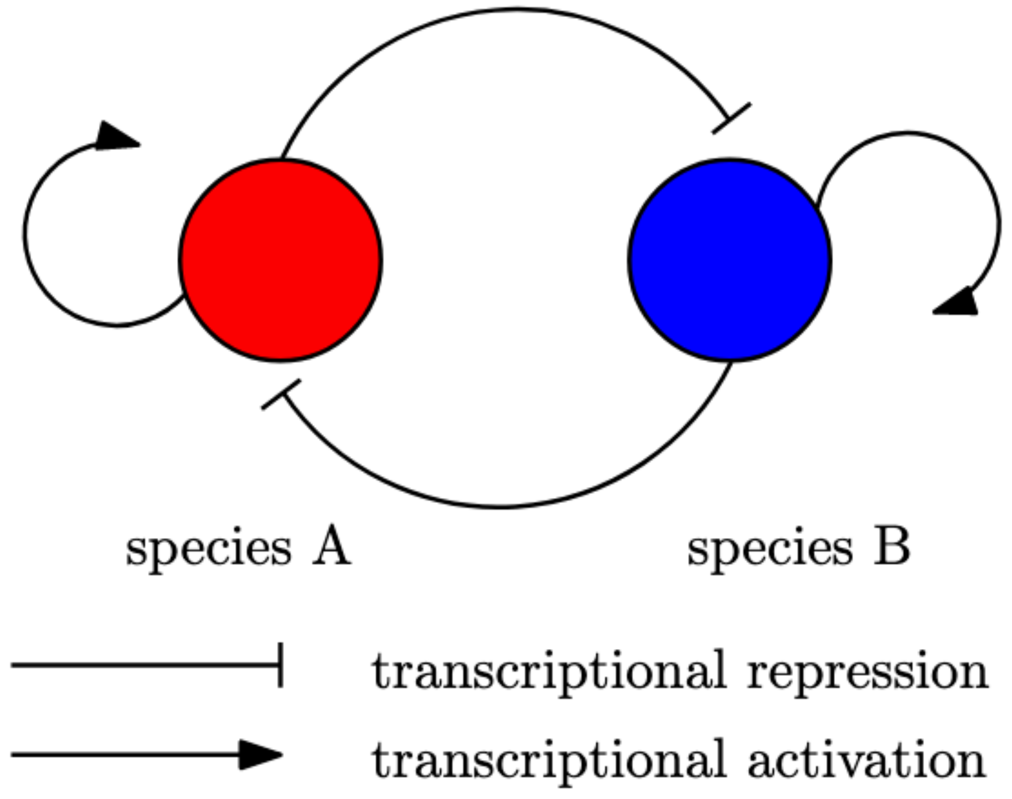

(a)

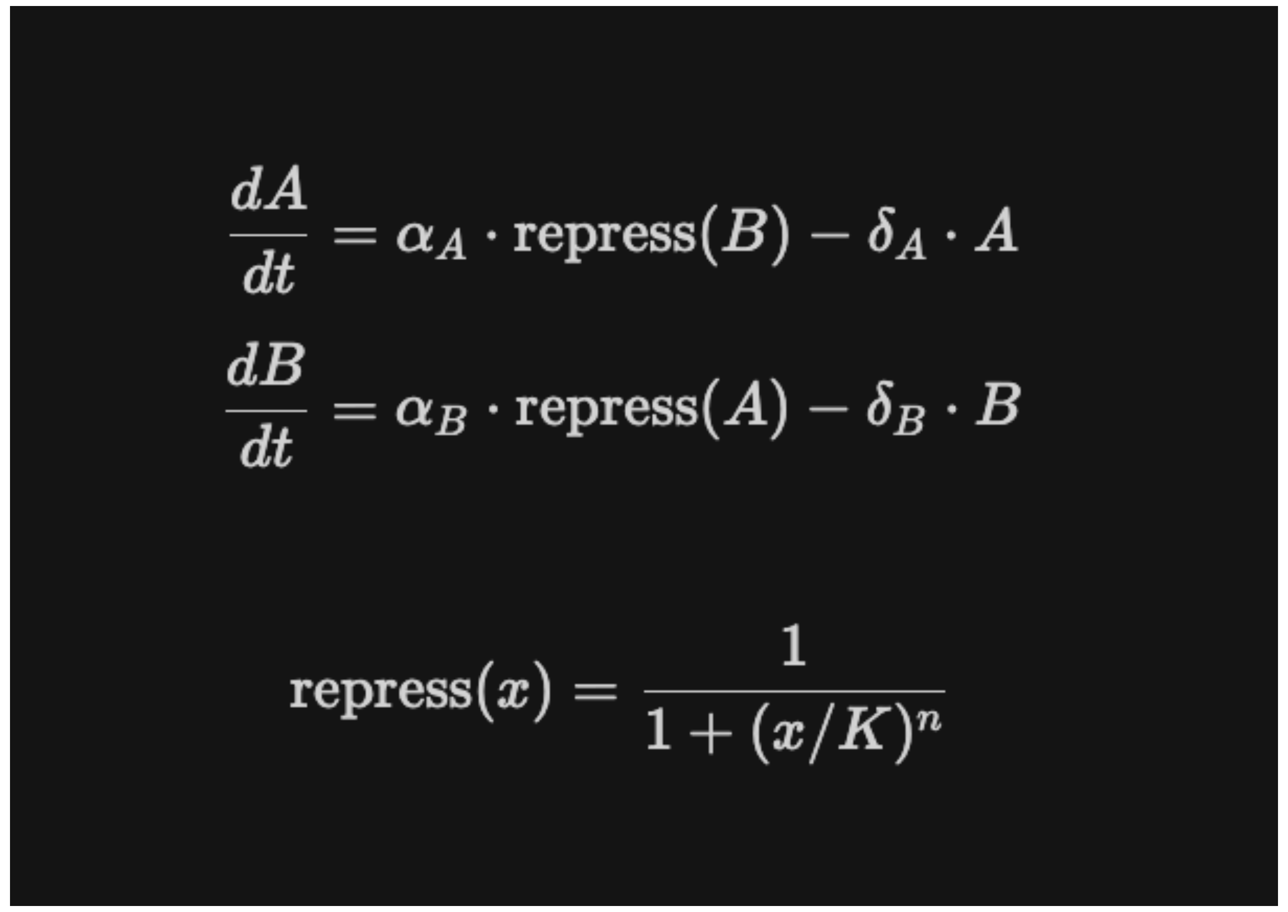

$$\frac{dA}{dt} = \alpha_A \cdot \text{repress}(B) - \delta_A \cdot A$$

$$\frac{dB}{dt} = \alpha_B \cdot \text{repress}(A) - \delta_B \cdot B$$

$$\text{repress}(x) = \frac{1}{1 + (x/K)^n}$$

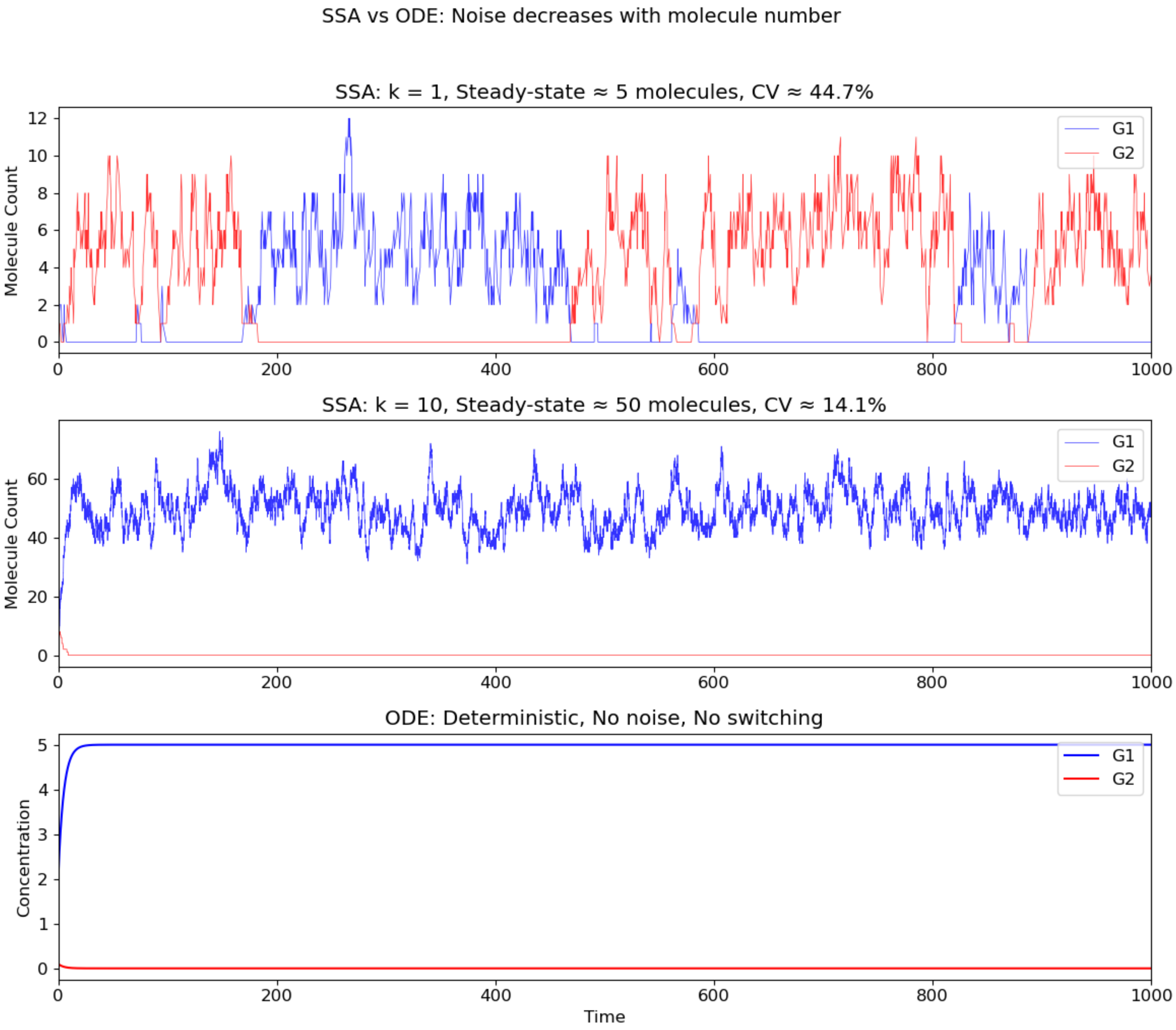

SSA vs ODE: Noise decreases with molecule number

SSA: k = 1, Steady-state ≈ 5 molecules, CV ≈ 44.7%

SSA: k = 10, Steady-state ≈ 50 molecules, CV ≈ 14.1%

ODE: Deterministic, No noise, No switching

# How to reproduce this fig?

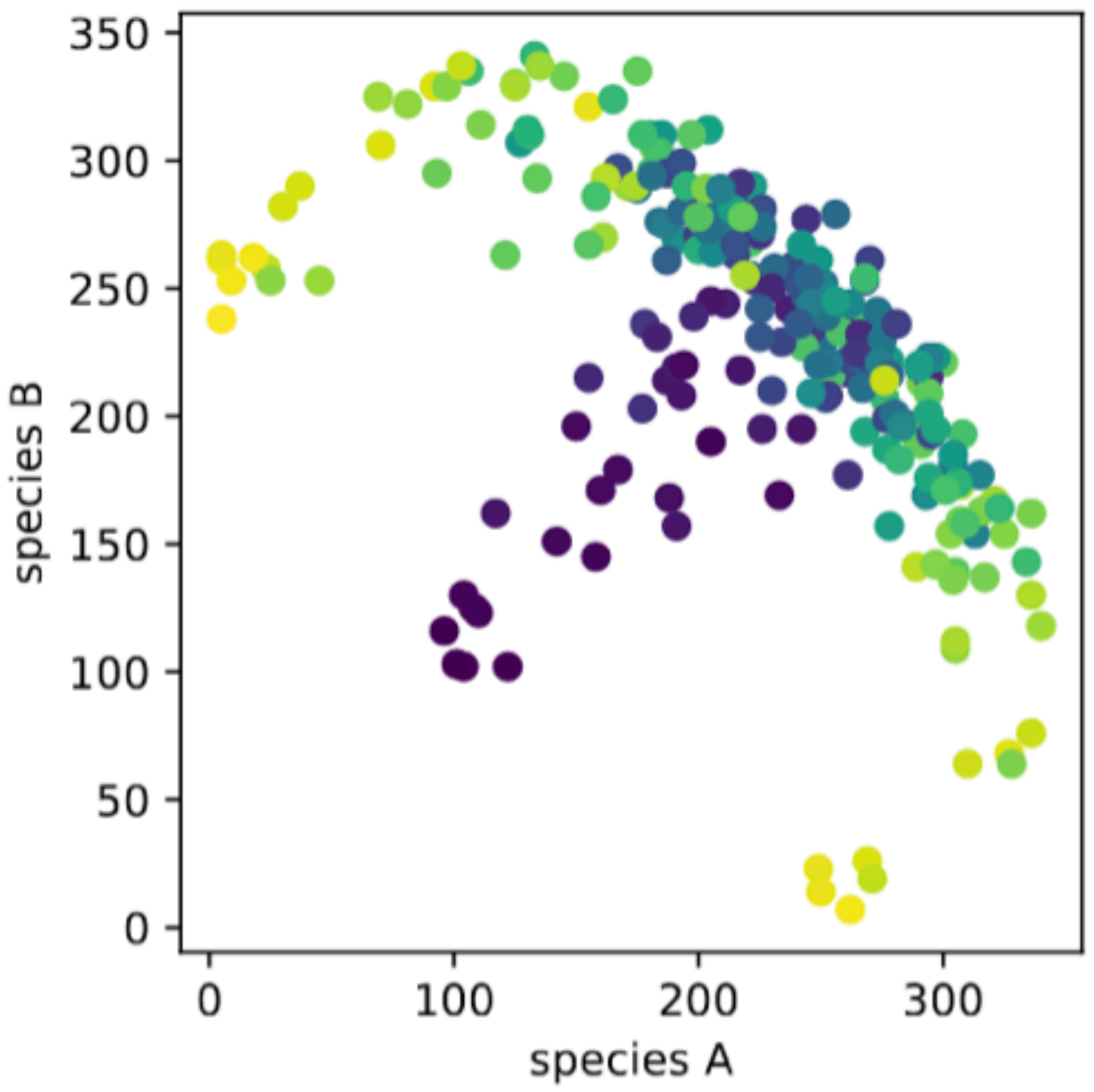

(c)

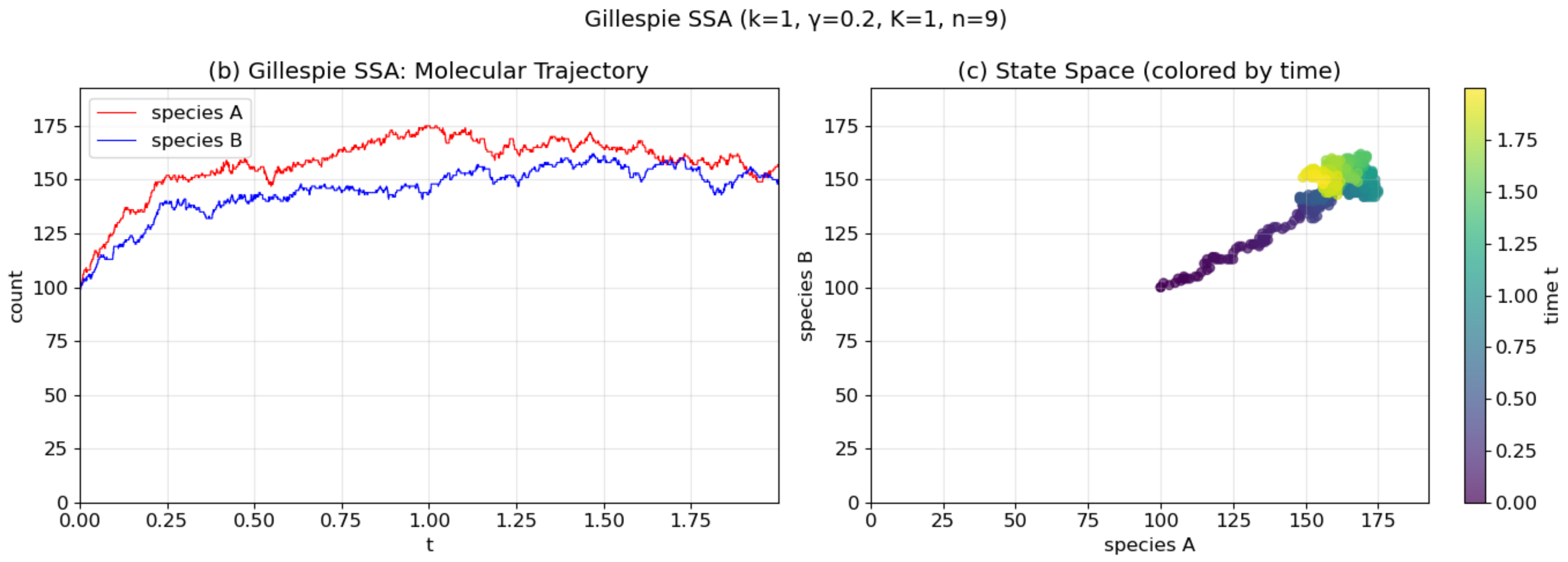

my result:

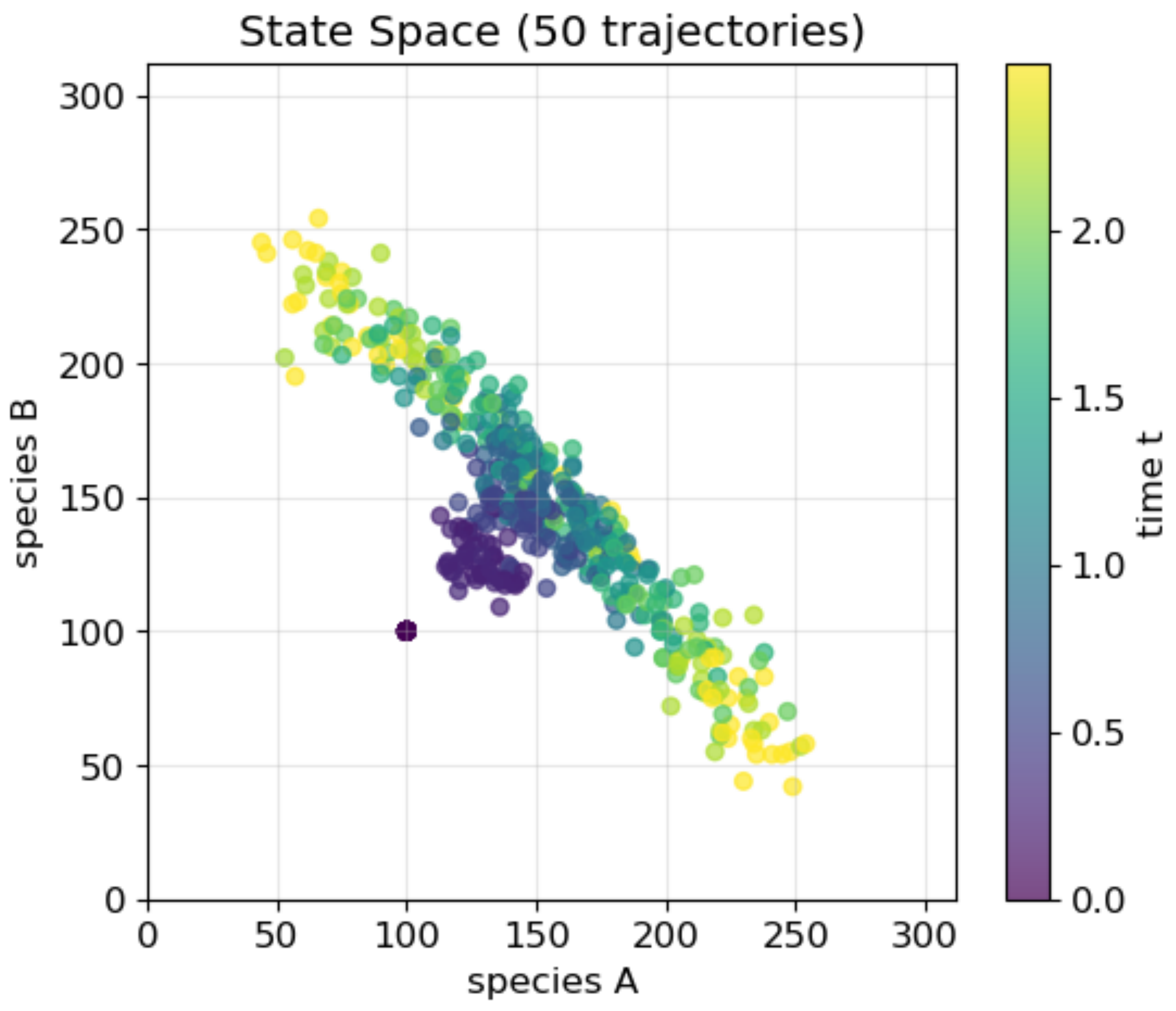

# Thank you